

NASA

Declassified by authority of NASA
Classification Change Notices No. 113
dated ** 6/22/67

TECHNICAL MEMORANDUM

ASSIGNED TO AUTOMATIC REGRADE
GROUP 4 AUTHORITY: LTR. NASA
STD. NOV. 12, 1962. SIGNED X-619
H.G. MAINES

9 [1961] 10

LOW-SPEED INVESTIGATION OF THE AERODYNAMIC CHARACTERISTICS
OF A VARIABLE-SWEEP SUPERSONIC TRANSPORT CONFIGURATION
HAVING A BLENDED WING AND BODY

By William C. Sleeman, Jr., and A. Warner Robins

NASA
Langley Research Center
Langley Air Force Base, Va.

ADVANCE
COPY

NOT TO BE INDEXED, REFERENCED, OR

This material contains information which, if disclosed, could be detrimental to the national defense. The transmission or revelation of its contents in any manner to an unauthorized person is prohibited by law.

NATIONAL AERONAUTICS AND SPACE ADMINISTRATION
WASHINGTON

FACILITY FORM 602

(ACCESSION NUMBER)

(THRU)

(NASA CR OR TMX OR AD NUMBER)

(CATEGORY)

IR

Declassified by authority of NASA
Classification Change Notices No. 43
Dated ** 6/23/67

DECLASSIFIED

NATIONAL AERONAUTICS AND SPACE ADMINISTRATION

TECHNICAL MEMORANDUM X-619

LOW-SPEED INVESTIGATION OF THE AERODYNAMIC CHARACTERISTICS
OF A VARIABLE-SWEEP SUPERSONIC TRANSPORT CONFIGURATION
HAVING A BLENDED WING AND BODY*

By William C. Sleeman, Jr., and A. Warner Robins

ABSTRACT

A wind-tunnel investigation was made to study the static longitudinal and lateral stability characteristics of a variable-sweep supersonic transport model. The tests were conducted at a Mach number of approximately 0.20 and the angle-of-attack range generally extended from -4° to 23° . The test Reynolds number based on the model reference chord was approximately 2.91×10^6 .

*Title, Unclassified.

[REDACTED]

DECLASSIFIED

NATIONAL AERONAUTICS AND SPACE ADMINISTRATION

TECHNICAL MEMORANDUM X-619

LOW-SPEED INVESTIGATION OF THE AERODYNAMIC CHARACTERISTICS
OF A VARIABLE-SWEEP SUPERSONIC TRANSPORT CONFIGURATION
HAVING A BLENDED WING AND BODY*

By William C. Sleeman, Jr., and A. Warner Robins

SUMMARY

Most of the investigation was concerned with the longitudinal stability characteristics of the model with the minimum sweep angle of 25° of the wing outer panel. A brief study was also made of the longitudinal characteristics of the model with sweep angles of the wing outer panels of 45° , 60° , and 80° . Lateral stability derivatives were obtained only for the maximum and minimum sweep angles. All tests were conducted at a Mach number of approximately 0.20 and the range of angles of attack generally extended from -4° to 23° . The test Reynolds number based on the model reference chord was approximately 2.91×10^6 .

The longitudinal stability characteristics of the basic model configuration having 25° sweepback were not satisfactory inasmuch as the stability was either neutral or unstable over the test angle-of-attack range above 5° . Several minor modifications to the model were investigated to attempt to improve the longitudinal stability; however, these modifications were not beneficial. Replacement of the highly swept leading edge on the wing inner panel of the basic model with a leading edge having an elliptical planform and extending the trailing edge of the wing outer panel greatly improved the longitudinal stability characteristics of the model with the 25° swept wing. The relatively small change in longitudinal stability with sweep angle for the basic model and the good longitudinal control characteristics evident throughout the test angle-of-attack range indicated that changes in control deflection required for trim throughout the sweep angle range would probably not be large.

The static directional stability of the basic model with sweep angles of 25° and 80° was fairly high up to an angle of attack of about 15° ; above this angle of attack there was a pronounced reduction in directional stability and the model with 25° sweepback became directionally unstable above an angle of attack of 21° .

*Title, Unclassified.

03:00:00

INTRODUCTION

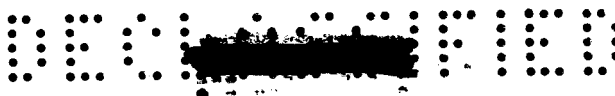
The National Aeronautics and Space Administration is conducting a research program directed toward the development of an efficient supersonic commercial air transport (SCAT) configuration. Past experience obtained in wind-tunnel studies of different types of supersonic-cruise bomber configurations (ref. 1) has indicated in general that trimmed lift-drag ratios required for Mach 3.0 cruise could be obtained for bomber configurations without incurring serious stability and control problems at supersonic speeds. Some of the results obtained on the bomber configurations at low speeds indicated, however, that some of the design features required for an efficient supersonic configuration were not compatible with good low-speed characteristics without further work on modifications tailored to improve the characteristics of each type of configuration. The research effort on supersonic transports has therefore been directed first toward the selection of several transport configuration concepts on the basis of attaining good low-speed stability and a high usable lift coefficient. Low-speed test results for a variable-sweep transport model designated as SCAT-6 are presented in reference 2. A discussion of some of the considerations underlying the use of variable sweep and a bibliography of reports concerned with variable-sweep airplane configurations is also given in reference 2.

L
1
6
2
2

The present paper presents results obtained in a low-speed investigation in the Langley 300-MPH 7- by 10-foot tunnel of a supersonic transport configuration. This model (designated SCAT-9) incorporated a blended wing concept in which the volume required for passengers and fuel was obtained primarily by thickening the wing and using large wing chords in the root sections of the wing in order to obtain this volume without incurring large penalties in supersonic wave drag. This design approach also permits the desired volume to be obtained with a lower ratio of total wetted area to wing planform area than could be obtained with an arrangement having a thin wing and the required volume in a separate fuselage. Details of some of the design considerations for the blended wing concept are presented in reference 3.

Other design aspects of the present model include the use of variable sweep on the outer panels of the wing. The design low-speed sweep angle was 25° and provision was made for a continuous increase in sweep to the maximum value of 80° . The configuration tested represented a four-engine airplane with a two-dimensional split-wedge inlet ducted to four turbofan engines buried in the rear of the fuselage. For the model tests, however, there was no airflow through the simulated engine pack. Longitudinal control was obtained by means of a variable-incidence horizontal tail approximately located on the wing chord plane extended.

SCAT-9



The present investigation was concerned primarily with an overall assessment of the longitudinal stability and control of the basic low-speed configuration of the model with 25° sweepback of the wing outer panels. These characteristics were obtained for an angle-of-attack range which extended from approximately -4° to 23° . Longitudinal characteristics of the model were also studied briefly with the wing outer panel set at sweep angles of 45° , 60° , and 80° , and lateral stability derivatives were determined for the 25° and 80° sweep positions of the wing. In addition to tests of the basic model, effects on the longitudinal characteristics of various modifications to improve the stability of the basic model were studied.

SYMBOLS

The data of this investigation are referred to the system of axes shown in figure 1. The lateral characteristics are referred to the body axes and the longitudinal characteristics are referred to the stability axes. Moment coefficients are given about a moment reference located at fuselage station 45.0. This reference location was 12.6 percent of the reference chord ahead of the wing-sweep pivot point. Inasmuch as there was no clear line of separation of the wing and body in the blended wing design, the reference area used in reduction of data to coefficient form was taken as the entire projected planform area of the model forward of the intersection of the root leading edge of the horizontal tail for the basic 80° sweep position of the wing outer panel. The reference span was taken as the span of the model with the wing outer panel sweptback 80° and the reference chord was obtained by dividing the reference area by the reference span. The variation of model area and span with angle of sweepback of the outer wing panel is given in table I.

C_L lift coefficient, $\frac{\text{Lift}}{qS}$

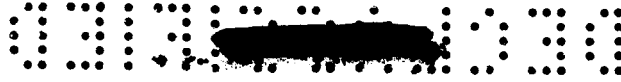
C_D drag coefficient, $\frac{\text{Total drag}}{qS} - C_{D,b}$

$C_{D,b}$ base-drag coefficient, $\frac{\text{Base drag}}{qS}$

C_m pitching-moment coefficient, $\frac{\text{Pitching moment}}{qS c_{\text{ref}}}$

C_l rolling-moment coefficient, $\frac{\text{Rolling moment}}{qS b_{\text{ref}}}$





$$C_{mC_L} = \frac{\partial C_m}{\partial C_L}$$

C_n yawing-moment coefficient, $\frac{\text{Yawing moment}}{qSb_{\text{ref}}}$

C_y side-force coefficient, $\frac{\text{Side force}}{qS}$

$$C_{L\alpha} = \frac{\partial C_L}{\partial \alpha}$$

$C_{l\beta}$ effective dihedral parameter, $\left(\frac{\Delta C_l}{\Delta \beta}\right)_{\beta=\pm 5^\circ}$

$C_{n\beta}$ directional stability parameter, $\left(\frac{\Delta C_n}{\Delta \beta}\right)_{\beta=\pm 5^\circ}$

$C_{y\beta}$ side-force parameter, $\left(\frac{\Delta C_y}{\Delta \beta}\right)_{\beta=\pm 5^\circ}$

b_{ref} reference span of wing ($\Lambda = 80^\circ$), 2.943 ft

c wing chord, ft

c_{ref} reference chord, $\frac{S}{b_{\text{ref}}}$, 2.644 ft

i_t incidence of horizontal tail with respect to fuselage reference line, positive for trailing edge down, deg

L/D lift-drag ratio

q free-stream dynamic pressure, lb/sq ft

S model reference area, 7.781 sq ft

X, Y, Z coordinate axes

α angle of attack of fuselage reference line, deg

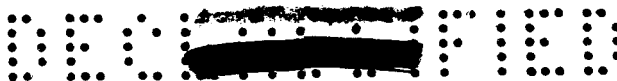
β angle of sideslip of fuselage reference line, deg

Λ angle of sweepback of leading edge of wing outer panels, deg

Subscript:

max maximum





MODEL DESCRIPTION

Basic Model

L
1
6
2
2


The general arrangement of the basic model tested in this investigation is shown in figure 2 and pertinent geometric characteristics are given in table I. This model was considered to be a $1/24$ -scale model of a supersonic transport airplane. The structural elements of the wing-body combination were made of aluminum and the external contour was formed from wood and plastic. The outer panels of the wing were constructed of aluminum and had Clark Y airfoil sections. The horizontal and vertical tails were constructed of $1/4$ -inch-thick aluminum flat plate with rounded leading edges and beveled trailing edges. The inboard panels of the wing had streamwise airfoil sections that corresponded closely to NACA 65A series airfoils and had an approximately parabolic distribution of thickness ratio with span out to the point that the thickness ratio had to increase in order to meet the structural thickness required at the wing-sweep pivot. The wing thickness at the 3.00-inch-span station was 5.45-percent chord and the thickness at the 11.00-inch-span station was 2.00-percent chord.

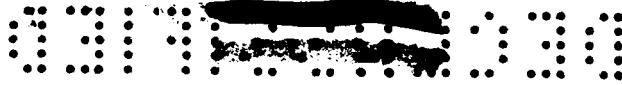
The present model was simplified in order to minimize problems of mounting the model to a single support strut passing through the bottom of the model and no provision was made for internal flow through the simulated engine pack. Therefore, the external shape of the engine pack did not conform to the shape for a two-dimensional split inlet designed for Mach number 3.0 operation but had a 20° wedge face rather than the proper geometric characteristics.

Modifications to the Basic Model

Several modifications were made to the basic configuration in attempts to improve the longitudinal stability characteristics of the model and details of these modifications are given in figure 3. Longitudinal characteristics of the model with a notch cut in the leading edge were studied briefly. This notch was $1/4$ inch wide and was inclined so that it was aligned with the free-stream direction when the model was at an angle of attack of approximately 10° .

Some tests were also made with the chord of the wing outer panels extended 0.40c ahead of the leading edge of the outer panels. This modification was accomplished by attaching a flat plate to the bottom of the airfoil section and fairing the upper surface between the basic and extended leading edge with modeling clay.





Modifications were made to the model to move the wing outer panels forward. For these tests, new outer panels were constructed of 3/16-inch aluminum sheet with a rounded leading edge and a blunt trailing edge and these panels were attached to the inboard panel in the location shown in figure 3.

Rather extensive modifications to the wing planform were made in the terminal stages of the testing and the leading edge of the inboard panels of the wing were given an elliptical planform as shown in figure 4. In this modification no attempt was made to reduce the wing thickness other than to round off the leading edge to give it an airfoil-like contour. Effects of a small fillet made of modeling clay and attached to the wing leading edge at the root were also determined. For all tests of the model with the elliptical planform leading edge, the trailing edge of the wing outer panel was extended 0.40c as shown in figure 4. Geometric characteristics of the modified model are given in table II.

L
1
6
2
2

TESTS AND CORRECTIONS

The present investigation was conducted in the Langley 300-MPH 7- by 10-foot tunnel at a dynamic pressure of 50 pounds per square foot which corresponds to an airspeed of approximately 141 miles per hour. The test Reynolds number based on the reference chord was approximately 2.91×10^6 .

Forces and moments acting on the model were measured by means of a 6-component internal strain-gage balance. This balance was attached to a central support strut which was mounted through the floor of the tunnel and the angle of attack and sideslip of the balance and model were remotely controlled. The test angle-of-attack range for most of the tests was from approximately -4° to 23° . Lateral stability derivatives were obtained from tests made at sideslip angles of $\pm 5^\circ$ throughout the angle-of-attack range.

Transition strips approximately 1/8 inch wide were placed on all lifting surfaces of the model at approximately 5 percent of the chord and were composed of carborundum particles having a nominal size of about 0.012 inch.

Blockage corrections were evaluated by the method of reference 4 and were applied to the dynamic pressure. Jet-boundary corrections to the angles of attack, drag coefficients, and pitching-moment coefficients obtained with the horizontal tail on were determined from the charts of reference 5. The following jet-boundary corrections were added to the data.



DECLASSIFIED

$$\Delta\alpha = 0.7334C_L$$

$$\Delta C_D = 0.0128C_L^2$$

$$\Delta C_m = 0.0060C_L$$

These corrections were applied to the data for all sweep angles tested inasmuch as changes in the correction factor at the lifting line varied with sweep angle (changes in wing span) in a manner that tended to compensate for changes in wing area with sweep angle. Corrections to the angle of attack arising from deflection of the strain-gage balance under load were also applied.

The drag coefficients have been adjusted to correspond to conditions of free-stream static pressure acting over the base of the model which included the engine-exit area and the fuselage area between the exits as shown in the rear view of the model in figure 2.

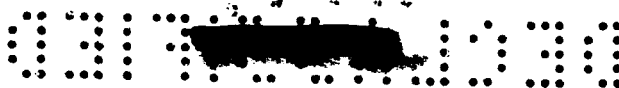
Corrections for the influence of the support strut on the model characteristics were not determined and the data therefore have not been corrected for support tares. Tests of other models of about the same size as the present model have indicated that an appreciable pitching-moment tare existed. This pitching-moment tare previously measured was essentially constant over the angle-of-attack range and amounted to a pitching-moment coefficient as large as 0.05 in some cases. The probable pitching-moment tares for the present model would be expected to affect the longitudinal trim and to have no effect on the longitudinal stability characteristics presented herein.

PRESENTATION OF RESULTS

An outline of the figure content presenting the results of this investigation is as follows:

Figure

Longitudinal characteristics of the basic model:	
$\Lambda = 25^\circ$	5
Photographs of tufts on the wing surface	6
$\Lambda = 45^\circ$	7
$\Lambda = 60^\circ$	8
$\Lambda = 80^\circ$	9
Wing outer panels removed	10
Summary of effects of wing sweep on stability and performance parameters	11



Figure

Effects of wing sweep on pitching moments	12
Lateral stability derivatives of the basic model:	
$\Lambda = 25^\circ$	13
$\Lambda = 80^\circ$	14
Modifications to the model with $\Lambda = 25^\circ$:	
Effect of dihedral in the horizontal tail	15
Effect of moving the wing outer panels forward	16, 17
Effect of notch and extended chord on the wing outer panel	18
Characteristics of model with elliptical planform leading edge	19
Effect of elliptical planform leading edge on pitching moments	20
Effect of tail dihedral and wing root fairing on model with elliptical planform leading edge	21

L
1
6
2
2

DISCUSSION

The present investigation was of an exploratory nature to determine whether this airplane arrangement would have acceptable low-speed characteristics inasmuch as the configuration was so different from other configurations previously tested that past experience could not be relied upon to assure that the arrangement would be satisfactory even with the flaps retracted. Past investigations of the application of high-lift devices have generally indicated that longitudinal stability problems with flaps deflected could be more easily avoided if the basic clean configuration without flaps had good longitudinal stability and control characteristics. Several modifications to the basic model were investigated therefore in attempts to improve the characteristics of the model in the low-sweep condition rather than investigating the lift capabilities of a flap system on a configuration that might be unsatisfactory from the standpoint of low-speed stability and control.

As noted previously, a large part of the present investigation was conducted on the configuration having the minimum sweep angle of 25° ; however, the coefficients presented herein are based on the geometric characteristics of the model with 80° sweep. The geometric characteristics of this configuration were used in the data reduction because the high-sweep cruise condition is the important configuration from the standpoint of selection of the airplane wing loading for efficient supersonic cruise flight. In using this basis of coefficient evaluation, a reduction in wing sweep (and attendant increase in wing area and aspect ratio) to the minimum sweep angle can be considered a means of increasing the airplane lift by changing its wing planform configuration for low-speed flight. This approach is consistent with conventional practice in the use of high-lift devices that increase the wing area by deflection of slotted flaps.





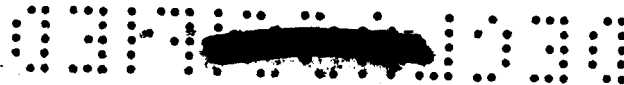
Longitudinal Characteristics of Basic Model

Model with 25° sweptback wing.-- Longitudinal characteristics of the basic model with the wing outer panels swept back 25° are presented in figure 5. These results show that the variation of lift coefficient with angle of attack was approximately linear up to about 10°. For higher angles of attack, the variation became nonlinear. This nonlinearity indicated some flow separation occurred on the wing; however, no pronounced wing stall with large losses in lift was evident. The lift-curve slope at low angles generally gave a good indication of the overall lifting characteristics of the model throughout the angle-of-attack range tested. This characteristic was not typical of the model for higher sweep angles and the differences in lift characteristics are discussed subsequently.

Maximum values of lift-drag ratio obtained were about 12.6 (fig. 5) without the horizontal tail and about 11.4 with the tail at 0° incidence. Deflection of the tail to provide longitudinal trim at positive angles of attack caused further reductions in maximum lift-drag ratios; however, at high-lift coefficients the effects of stabilizer setting on lift-drag ratios were small. This small effect would imply that changes in lift-drag ratio resulting from trimming the model at high-lift coefficients would therefore be small. The apparent insensitivity of lift-drag ratios to stabilizer setting at high lift may in part be due to the fact that increasing positive deflection of the tail was required for trim because of the instability that existed at high angles of attack. This rather extensive region of instability decreases the significance of the trim characteristics inasmuch as this instability would not be acceptable for an airplane of this type.

Pitching-moment characteristics of the model presented in figure 5 show that the wing-body configuration was neutrally stable up to a lift coefficient of about 0.28. Above this lift coefficient there was a large forward movement of the aerodynamic center and for angles of attack above about 15° the pitching-moment slope C_{mC_L} reached a value of approximately 0.18. This large loss in stability was also reflected in the pitching moments with the tail on and for lift coefficients above 0.60 ($\alpha = 10^\circ$), the overall pitching-moment slope with the tail on ($i_t = 10^\circ$) was about $C_{mC_L} = 0.07$. These results indicate that the horizontal tail provided a stabilizing contribution throughout the test angle-of-attack range and that the basic stability problem for this model was therefore associated with the wing-body characteristics.

Pitching-moment characteristics of the basic model with different stabilizer deflections presented in figure 5 show that the longitudinal control effectiveness was good throughout the angle-of-attack range tested and that the effectiveness at high angles of attack was in most cases greater than at an angle of attack of 0°.



Flow studies on model with 25° sweptback wing.- Inasmuch as the longitudinal stability problems of the basic model appeared to be in the wing characteristics, some studies of the flow over the wing were made by tufts attached to the model surface. Some of the photographs obtained in this study are presented in figure 6 to illustrate the flow characteristics over the surface of the model at several angles of attack.

The tuft photographs show that the smooth flow that existed near an angle of attack of 0° was no longer evident at a fairly low angle of attack ($\alpha = 4.33^\circ$). The formation of a leading-edge vortex with attendant spanwise flow along the highly swept leading edge of the wing inner panel was indicated at $\alpha = 4.33^\circ$. This flow disturbance at the leading edge appeared to originate at about the half span of the wing inner panel and the point of origin moved inboard as the angle of attack increased. The region of disturbed flow appeared to fan out over the wing surface aft of the leading edge and to progress outboard over the wing outer panel as the angle of attack increased. The tuft photographs of figure 6 are helpful in explaining why the pitching moments of the wing-body configuration showed a loss in stability above an angle of attack of 4°. Apparently there was a reduction in the proportion of lift load carried on the wing outer panel as the angle of attack was increased while the inboard part of the wing continued to be effective in producing lift. Both of these effects would, of course, contribute to an increase in the nose-up moments of the model. Test results obtained with the wing outer panels removed, presented in figure 10, also show that the wing inner panel was effective in producing lift at high angles of attack as evidenced by the fact that the lift-curve slope at an angle of attack of 10° was approximately twice the slope near an angle of attack of 0°.

L
1
6
2
2

Effects of wing sweep.- The basic data from which the effects of wing sweep on longitudinal stability may be obtained are presented in figures 5 and 7 to 9 and these results are summarized in figures 11 and 12. The variation of longitudinal stability at low lift with angle of sweepback of the wing outer panels is shown in figure 11. These results show that there was little change in C_{mC_L} with sweep angle up to about

45°. For sweep angles greater than 45° a progressive loss in stability was indicated, both with the horizontal tail on and off. The loss of stability in changing from 45° sweep to 80° sweep with the tail on was, however, about half of that obtained for the tail-off configuration. This forward shift in center of pressure with increasing sweep should be beneficial for supersonic flight and would result in less change in stability with Mach number providing it can be controlled at subsonic speeds.

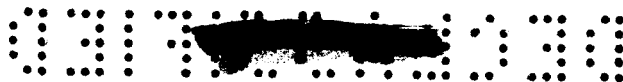
The pitching-moment data for the model were very nonlinear, especially at the lower sweep angles, and a better overall comparison



of the data can therefore be obtained from a comparison of the pitching-moment curves rather than from slopes taken over a restricted lift range. This comparison of pitching-moment curves is presented in figure 12, the tail-on and tail-off results being given separately. These results show large differences in the tail-off characteristics for the different sweep angles and the abrupt changes in stability at low lift became progressively smaller as the sweep angle increased above 45° . For the 80° swept configuration there was comparatively little change in stability with lift coefficient, both with the tail on and off. Furthermore, there was very little effect of sweep on the absolute value of the pitching moments with the tail on at high angles of attack. This very small effect of sweep on the pitching moments at high angles of attack and the absence of large effects at other angles (pitching-moment increment due to sweep at $C_L = 0.5$ was less than that given by 10° deflection of the tail on the 25° swept configuration) suggests that changes in control deflection required for longitudinal trim through the sweep-angle range would not be large for this configuration.

Effects of sweep of the wing outer panel on the wing-body lift-curve slopes as obtained both from estimates and test data are shown in figure 11. The estimates were made by use of the theoretical expression for lift-curve slope given in reference 6 which defined C_{L_α} in terms of the aspect ratio and sweep of the half-chord line for ordinary swept wings having linear taper. A procedure has been developed for extending this method to swept wings having a composite wing planform or nonlinear planform taper and this procedure is presented in reference 7. This method for estimating C_{L_α} involves determination of an effective half-chord sweep for a wing planform having nonlinear taper by a simple area weighting of the cosines of the local half-chord sweep angles across the wing span. This method of reference 7 has been found to be fairly reliable for a wide range of composite swept-wing planforms. The agreement between estimated and experimental lift-curve slopes for the present model (fig. 11) is only fair at low-sweep angles and becomes more reliable at the higher sweep angles. Inasmuch as the present wing planform differed so radically from a normal swept wing, especially at the lowest sweep angle, close agreement between estimated and experimental lift-curve slopes would not necessarily be expected.

The variation with wing outer panel sweep of maximum lift-drag ratios and lift coefficient for maximum lift-drag ratio is also shown in figure 11(a). Values of maximum lift-drag ratio with the tail on varied from 11.0 to about 6.2 as the sweep was increased from 25° to 80° . In order to obtain an indication of the amount of leading-edge suction the model may have experienced near $(L/D)_{\max}$, experimental results for the wing body have been compared in figure 11(b) with estimates of $(L/D)_{\max}$ obtained for the assumptions of zero and full leading-edge suction. The theoretical value of drag coefficient at



zero lift used in the estimates was obtained from a plot of the variation of experimental drag coefficients with C_L^2 . The comparison presented in figure 11(b) shows that the model developed over half of the full leading-edge suction at all sweep angles. The results of reference 8 indicate the possibility that, for Reynolds numbers corresponding to the full-scale airplane, a higher percentage of full leading-edge suction may be realized than the model test data indicate.

Lateral Stability Derivatives of Basic Model

Inasmuch as significant longitudinal stability problems on the basic model became apparent early in the course of testing, only a cursory study of the lateral stability characteristics of the model was made. Characteristics of the model with 25° sweep (fig. 13) show an abrupt change in the variation with angle of attack of the effective dihedral parameter $C_{l\beta}$ above an angle of attack of about 6.5°. This change in slope which is followed eventually by a reversal in the sign of $C_{l\beta}$ was probably caused by the same flow breakdown on the wing outer panel that caused the loss in longitudinal stability at low angles of attack. This observation appears to be consistent with the results for the 80° swept wing (fig. 14) in that the variation in both $C_{l\beta}$ and pitching moment with angle of attack was nearly linear up to the highest angle of attack tested. Apparently small changes in wing sweep relative to the free-stream direction, caused by sideslipping the wing, had a critical effect on the flow over the model with 25° sweep whereas the 80° sweep was so high that the ±5° sideslip had little of the critical effect noted for the low-sweep condition.

The directional stability of the model at low angles of attack was fairly high for both sweep angles (figs. 13 and 14); however, there was a loss in stability at the highest angles of attack. The model with 25° sweep became directionally unstable at angles of attack above approximately 21° whereas the stability at $\alpha = 21^\circ$ of the model with 80° sweep decreased to slightly less than half of the value at an angle of attack of 0°. The cause of this loss in directional stability for both sweep angles is believed to be a loss in the contribution of the vertical tail. Tail-off characteristics obtained for the 80° swept configuration (fig. 14) show that the wing-body directional instability did not change appreciably over the angle-of-attack range whereas the vertical-tail contribution to both $C_{n\beta}$ and $C_{y\beta}$ decreased above an angle of attack of 15°. Results for the model with 25° sweep showed a large reduction in $C_{y\beta}$ at high angles of attack which, when considered with the directional instability, would indicate that the vertical tail was losing its contribution to stability.

Modifications to Basic Configuration

The longitudinal stability problems encountered on the basic configuration with the 25° swept wing prompted an investigation of several modifications to the model for the purpose of alleviating these problems. Several different approaches were taken, most of which involved changes to the basic wing and results are not presented for all the modifications tested such as, for example, a large fence located at the sweep pivot and several planform discontinuities at the leading-edge juncture of the wing inner and outer panels. Some of the results from the modification studies are presented to show some unsuccessful approaches as well as the modification that did improve the characteristics of the model.

Effect of tail dihedral.- The model had means provided for easily changing the tail dihedral from 0° to -15° and this modification was investigated to determine whether an improvement in tail contribution could be realized to overcome the wing-body instability of the model. The results of this study presented in figure 15 show no significant effect of -15° dihedral in the tail. Apparently, the rather small vertical displacement accompanying -15° dihedral was not sufficient to locate the tail in a more favorable flow region. Perhaps the use of more dihedral or lowering the tail root would be required to locate the tail in a position to provide satisfactory longitudinal stability. Test data on SCAT-6, for example (see ref. 2) demonstrated that lowering the horizontal tail was very beneficial in counteracting adverse stability characteristics of the wing-body configuration. This modification, however, could not be easily made on the present model because of the engine exit configuration used.

Effects of moving the wing outer panels forward.- Aerodynamic characteristics of the model with the wing outer panels moved forward approximately 3.5 inches (see fig. 3) are presented in figure 16. The most obvious effect of this modification was the expected overall decrease of stability throughout the lift range caused by moving the outer, more rearward lifting surface closer to the moment reference. Inasmuch as the primary purpose of all the modifications studied was to eliminate the unfavorable change in stability with lift, the results with modifications should be compared with the basic data for approximately the same stability level at low lift. The data therefore have been recomputed about new moment reference locations in order to give a more reasonable amount of stability at moderate lift coefficients (up to about $C_L = 0.4$) for both the basic and modified model with 10° stabilizer setting. These recomputed results presented in figure 17 show that moving the outer panels forward had a beneficial effect on the tail-on pitching moments, particularly for lift coefficients above 0.80. Although this modification had an aerodynamic benefit, the possible problem of weight and balance for an airplane might make it difficult, if not impossible, to move the center of gravity forward enough to provide

REF ID: A60000

adequate stability even at low lift for the modified configuration. For this reason, modifications which did not affect or improve the low-lift stability would be much more desirable.

Effect of notch and extended chord.- Two modifications which were not expected to have a large effect on the low-lift stability of the model were investigated and the results are presented in figure 18. A notch in the leading edge of the inner panel, perpendicular to the plane of symmetry (see fig. 3) was cut in the wing for the purpose of venting the upper surface of the highly swept wing inner panel in an attempt to delay or moderate the leading-edge flow on this panel. For the other modification, the leading edge of the wing outer panels was extended 0.40c in order to increase the area of these panels. The data presented in figure 18 show that neither of these modifications effected significant improvement in the longitudinal stability of the model.

L
1
6
2
2

Model With Elliptical Planform Leading Edge

The results presented thus far have indicated that satisfactory characteristics of the model could not easily be obtained by means of minor modifications and it therefore would appear that a more extensive modification would be required. Inasmuch as the problem appeared to be associated with the highly swept wing inner panel, the forward portion of this panel was removed and the leading edge of the modified inner panel was given an elliptical planform as shown in figure 4. In addition to this change in the model, the trailing edge of the wing outer panels was extended 0.40c.

Effect of planform modification.- A comparison of the lift characteristics of the basic model (fig. 5) and the modified model (fig. 19) shows an appreciable difference in the shape of the lift curve at moderate and high angles of attack. The basic model showed no pronounced overall decrease in lift-curve slope above an angle of attack of 10° whereas the modified model showed a marked decrease in lift slope above an angle of attack of approximately 10° . This change in lift characteristics is believed to be caused primarily by the removal of the wing area which existed, for the basic model, ahead of the modified leading edge and contributed appreciably to the instability of the basic model.

Values of the maximum lift-drag ratio for the basic model (fig. 5) were appreciably improved by the modification. (See fig. 19.) The increment in maximum lift-drag ratio was about 2.0 for both the tail-off and the 0° stabilizer setting. The amount of contribution to this increment of the added area to the wing outer panels was not determined; however, it might be expected that this area added to the rear part of the wing would have some beneficial effect. The improvement in maximum

REF ID: A60000

CONFIDENTIAL

lift-drag ratio for the modified model is believed to be largely attributed to a favorable effect of the elliptical planform leading edge on the drag due to lift of the modified model. At high lift, the modified model had lower values of lift-drag ratio than the basic model because the lower lift-curve slope at high angles required a higher angle of attack to produce a given lift coefficient.

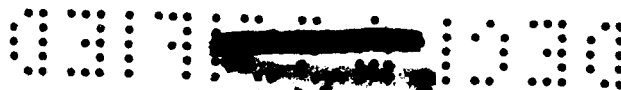
L
1
6
2
2

Pitching-moment characteristics for the modified model presented in figure 19 are referred to the same moment reference point as for the basic model. These results show a marked improvement in the variation of stability throughout the lift range compared with the basic model. The low-lift stability level was, however, very high as a result of removing wing area ahead of the moment reference and adding wing area to the rearward outer panels. The pitching-moment characteristics for this case, as before, should have approximately the same stability level with the tail on in order to assess properly the effects of the modification. These data have therefore been recomputed and the results are presented in figure 20. Unlike the previous instance, with the outer panels shifted forward, the moment reference for the modified model was shifted rearward about 9 percent of the reference chord; for the basic model the moment reference was shifted forward about 5 percent of the average chord as before.

The data presented in figure 20 show a marked improvement in the nature of the pitching-moment variation for the modified model, both with the tail on and off. Pitching moments for the modified model are considered much more desirable than those for the basic configuration, even though both show regions of instability or neutral stability at moderate lift. The important benefit gained was in the fact that the instability that did occur for the modified model was not severe; it occurred over a relatively small lift-coefficient range and was followed by a region of very high stability. This large increase of stability at high lift would be expected to prevent large unintentional excursions in angle of attack or excess normal accelerations for an airplane having these characteristics. Pitching moments for the basic model, on the other hand, appear highly undesirable because the region of instability and neutral stability is very extensive ($C_L = 0.40$ to 1.25) and this condition could cause large angle-of-attack and normal-acceleration overshoot for an airplane if this region were entered with an appreciable pitching rate.

Modifications to model.- Two modifications to the model with the elliptical planform leading edge were investigated and the results from this study are presented in figure 21. The model was tested with the horizontal tail set at -15° dihedral for the purpose of attempting to alleviate the moderate instability encountered on the model. These results indicated that -15° dihedral in the horizontal tail would not accomplish this purpose.

CONFIDENTIAL



The wing root fairing shown in figure 3 was tested on the model to determine whether some of the area removed in the leading-edge modification could be replaced without encountering the longitudinal stability difficulties of the basic configuration. The use of large chords near the root of the wing was considered desirable from the standpoint of good supersonic drag characteristics by keeping the thickness ratio as low as possible where the wing blended into the body. The data presented in figure 21 showed no effect of the wing-root fairing on stability of the model up to a lift coefficient of about 0.70 where the instability was slightly more pronounced. For lift coefficients above about 0.80 there was again essentially no effect of the wing root fairing on stability; however, the lift at a given angle of attack was increased somewhat. These results indicate therefore that some increase in the chords at the leading edge near the wing root can be tolerated from the standpoint of low-speed longitudinal stability; however, the amount of increase that could be accepted was not determined in these tests.

CONCLUSIONS

The following conclusions may be drawn from a low-speed investigation of the aerodynamic characteristics of a variable-sweep transport airplane configuration having a blended wing and body.

1. The longitudinal stability characteristics of the basic model with the wing outer panel sweptback 25° were unsatisfactory because the stability with the tail on was either neutral or unstable over the angle-of-attack range above about 5° .
2. Moving the wing outer panels forward had a marked beneficial effect on the variation of longitudinal stability with lift. This movement of the wing, however, caused an appreciable loss in the overall stability level which would require a fairly large forward movement of the center of gravity to provide a reasonable amount of stability at low lift.
3. Replacing the highly swept leading edge of the wing inboard panel with an elliptical planform leading edge and extending the trailing edge of the wing outer panels 40 percent of the chord greatly improved the longitudinal stability of the model to the extent that the characteristics would appear to be satisfactory. This modification also provided an increase in the maximum lift-drag ratio of about 2.0 with the tail off and with 0° stabilizer setting.
4. Increasing the sweep angle from 45° to 80° caused an appreciable loss of stability for the wing-body configuration; however, this loss in stability was greatly reduced with the horizontal tail on. Consideration



SECRET

17

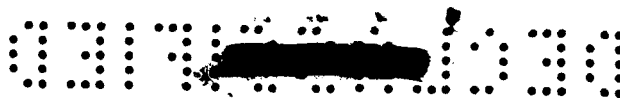
of the stability changes with sweep angle and the good control effectiveness throughout the angle-of-attack range suggests that changes in control deflection required for longitudinal trim through the sweep angle range would not be large for the basic configuration.

5. Directional stability of the model with the 25° and 80° swept outer panels was fairly high at low angles of attack; however, there was an appreciable loss in directional stability for angles of attack above about 15° . The 25° swept configuration became directionally unstable at an angle of attack above 21° whereas the stability of the 80° swept configuration at an angle of attack of 21° had decreased to only about half of the value at an angle of attack of 0° .

6. The effective dihedral of the basic model with 25° sweep began to decrease with increasing angle of attack at about the same angle that the longitudinal stability showed a marked decrease and showed a reversal in sign near an angle of attack of 23° . The model with 80° sweep, on the other hand, showed a variation of effective dihedral with angle of attack that continued to increase up to the highest angle of attack tested.

Langley Research Center,
National Aeronautics and Space Administration,
Langley Air Force Base, Va., September 9, 1961.

SECRET



REFERENCES

1. Baals, Donald D., Toll, Thomas A., and Morris, Owen G.: Airplane Configurations for Cruise at a Mach Number of 3. NACA RM L58E14a, 1958.
2. Vogler, Raymond D., and Turner, Thomas R.: Exploratory Low-Speed Wind-Tunnel Stability Investigation of a Supersonic Transport Configuration With Variable-Sweep Wings. NASA TM X-597, 1961.
3. Robins, A. Warner, Harris, Roy V., Jr., and Jackson, Charlie M., Jr.: Characteristics at Mach Number of 2.03 of a Series of Wings Having Various Spanwise Distributions of Thickness Ratio and Chord. NASA TN D-631, 1960. L
1
6
2
2
4. Herriot, John G.: Blockage Corrections for Three-Dimensional-Flow Closed-Throat Wind Tunnels, With Consideration of the Effect of Compressibility. NACA Rep. 995, 1950. (Supersedes NACA RM A7B28.)
5. Gillis, Clarence L., Polhamus, Edward C., and Gray, Joseph L., Jr.: Charts for Determining Jet-Boundary Corrections for Complete Models in 7- by 10-Foot Closed Rectangular Wind Tunnels. NACA WR L-123, 1945. (Formerly NACA ARR L5G31.)
6. Polhamus, Edward C., and Sleeman, William C., Jr.: The Rolling Moment Due to Sideslip of Swept Wings at Subsonic and Transonic Speeds. NACA TN D-209, 1960. (Supersedes NACA RM L54L01.)
7. Spencer, Bernard, Jr.: A Simplified Method for Estimating Subsonic Lift-Curve Slope at Low Angles of Attack for Irregular Planform Wings. NASA TM X-525, 1961.
8. Trescot, Charles D., Jr., and Spencer, Bernard, Jr.: Effect of Reynolds Number on the Low-Speed Longitudinal Aerodynamic Characteristics of Two Variable-Wing-Sweep Airplane Configurations. NASA TM X-434, 1961.



DECLASSIFIED

TABLE I
GEOMETRIC CHARACTERISTICS OF THE PLANFORM OF THE
BASIC MODEL CONFIGURATION

	Inner panel alone	$\Lambda = 25^\circ$	$\Lambda = 45^\circ$	$\Lambda = 60^\circ$	$\Lambda = 80^\circ$
Wing:					
Total area, sq ft	6.889	8.151	8.017	7.917	7.781
Total span, ft	2.250	5.442	4.810	4.108	2.943
Aspect ratio	0.735	3.63	2.88	2.13	1.11
Average chord, ft	3.062	1.498	1.667	1.927	2.644
Outer panel area, sq ft	-----	2.102	1.968	1.868	1.733
Effective sweep of half chord, deg	50.5	48.1	51.2	53.6	58.6
Horizontal tail (exposed planform of one panel):					
Area, sq ft					0.578
Span, ft					0.634
Leading-edge sweepback, deg					60
Vertical tail (exposed planform):					
Area, sq ft					0.962
Span, ft					0.956
Leading-edge sweepback, deg					70

0317: [REDACTED] :030

• • • •

TABLE II
 GEOMETRIC CHARACTERISTICS OF THE PLANFORM OF THE MODEL WING
 HAVING THE ELLIPTICAL LEADING EDGE ON THE INNER PANEL
 AND EXTENDED TRAILING EDGE ON THE OUTER PANEL

$$[\Lambda = 25^\circ]$$

	Planform assumption 1 (a)	Planform assumption 2 (b)
Area, sq ft	8.550	7.765
Span, ft	5.442	5.442
Aspect ratio	3.463	3.814
Average chord, ft	1.5712	1.427
Outer panel area, sq ft	2.263	2.263
Effective sweep of half chord, deg	38.63	34.29

^aIncludes planform area of fuselage ahead of the wing.

^bWing leading edge of inner panel extended to plane of symmetry and excludes planform area of fuselage ahead of wing.

[REDACTED]

L
1
6
2
2

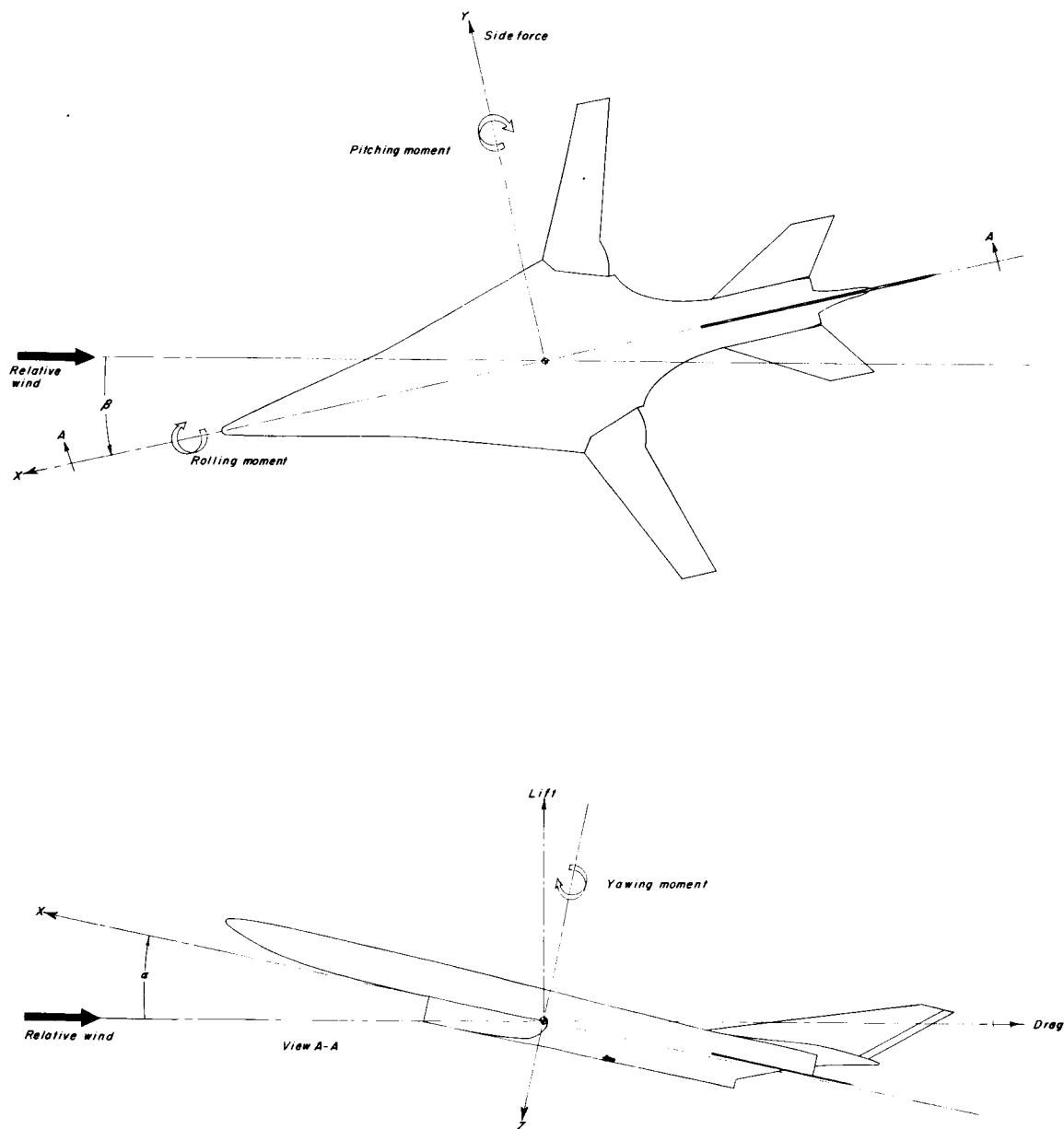
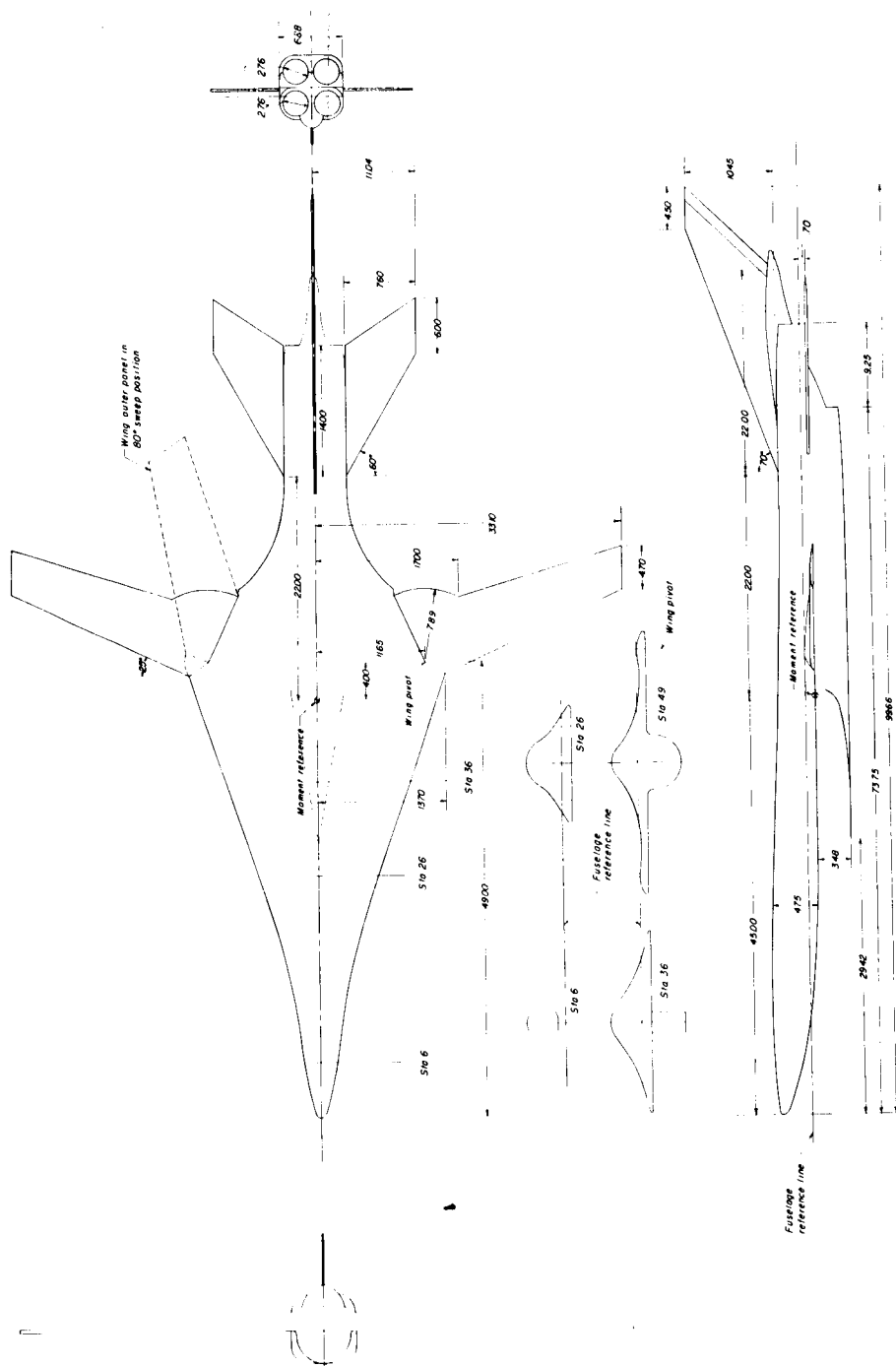


Figure 1.- System of axes used in presentation of the data.



DECLASSIFIED

L-1622

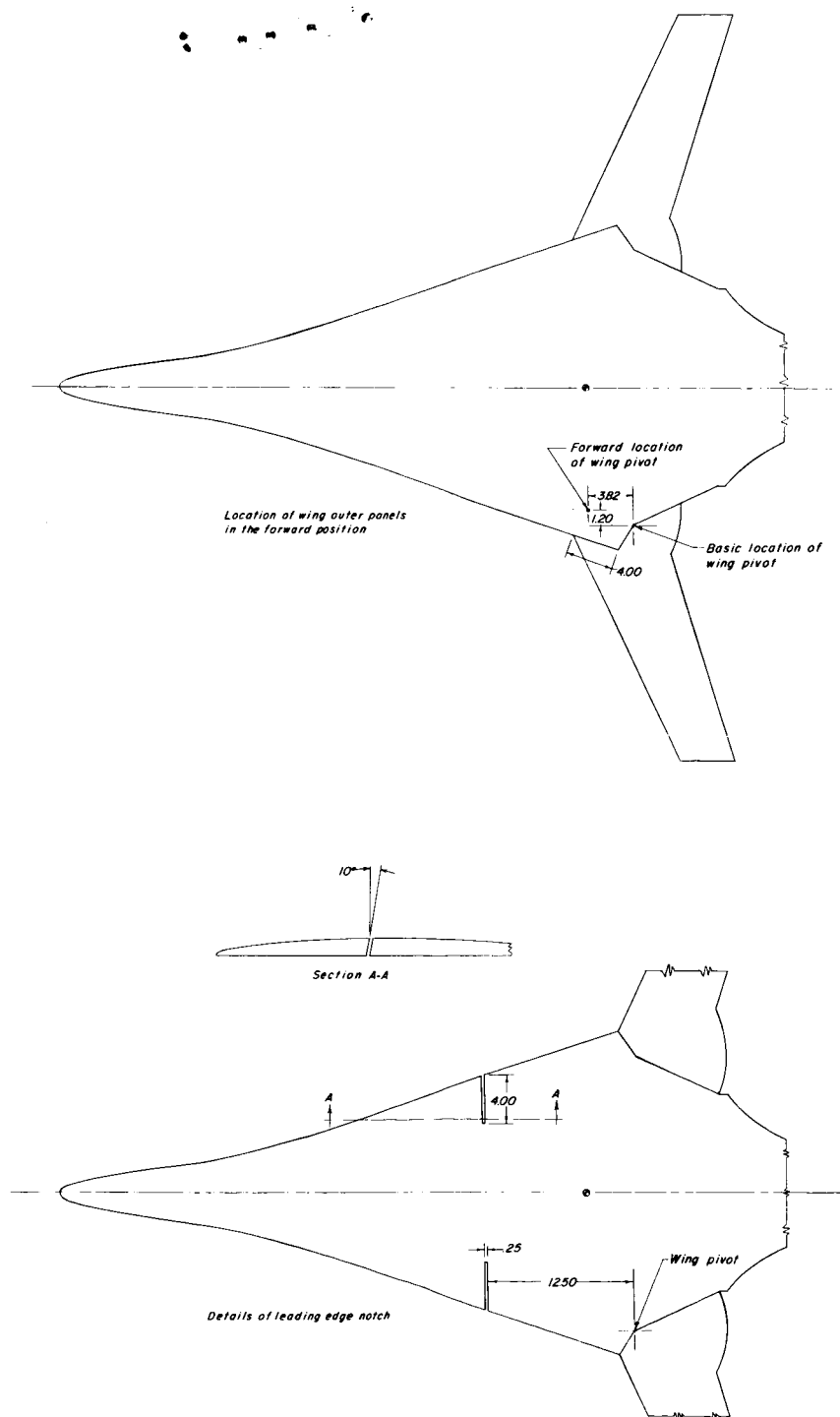


Figure 3.- Details of modifications to basic model configuration.

037-1030

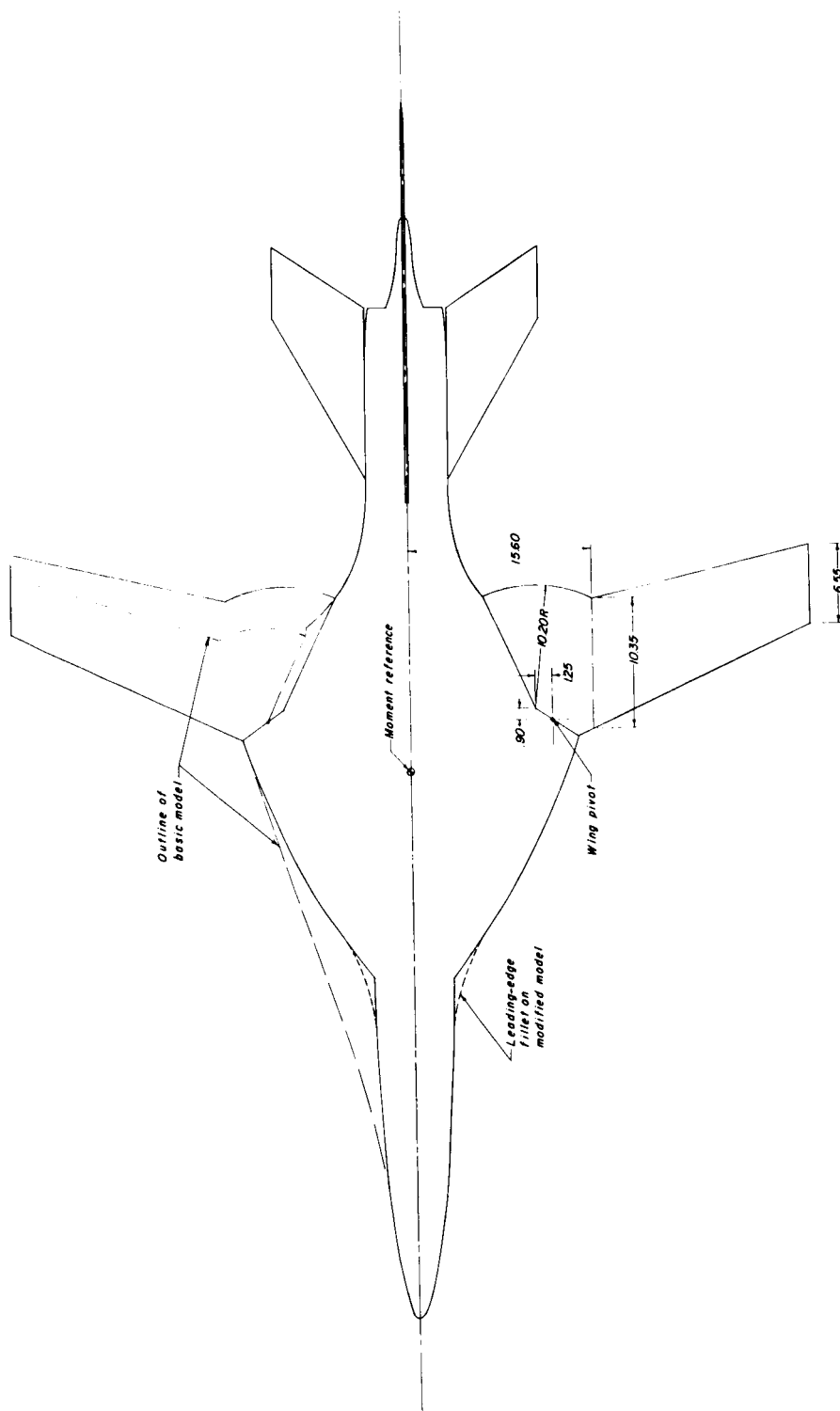


Figure 4.- Plan view of the modified model having an elliptical leading edge on the wing inner panel.

I-1622

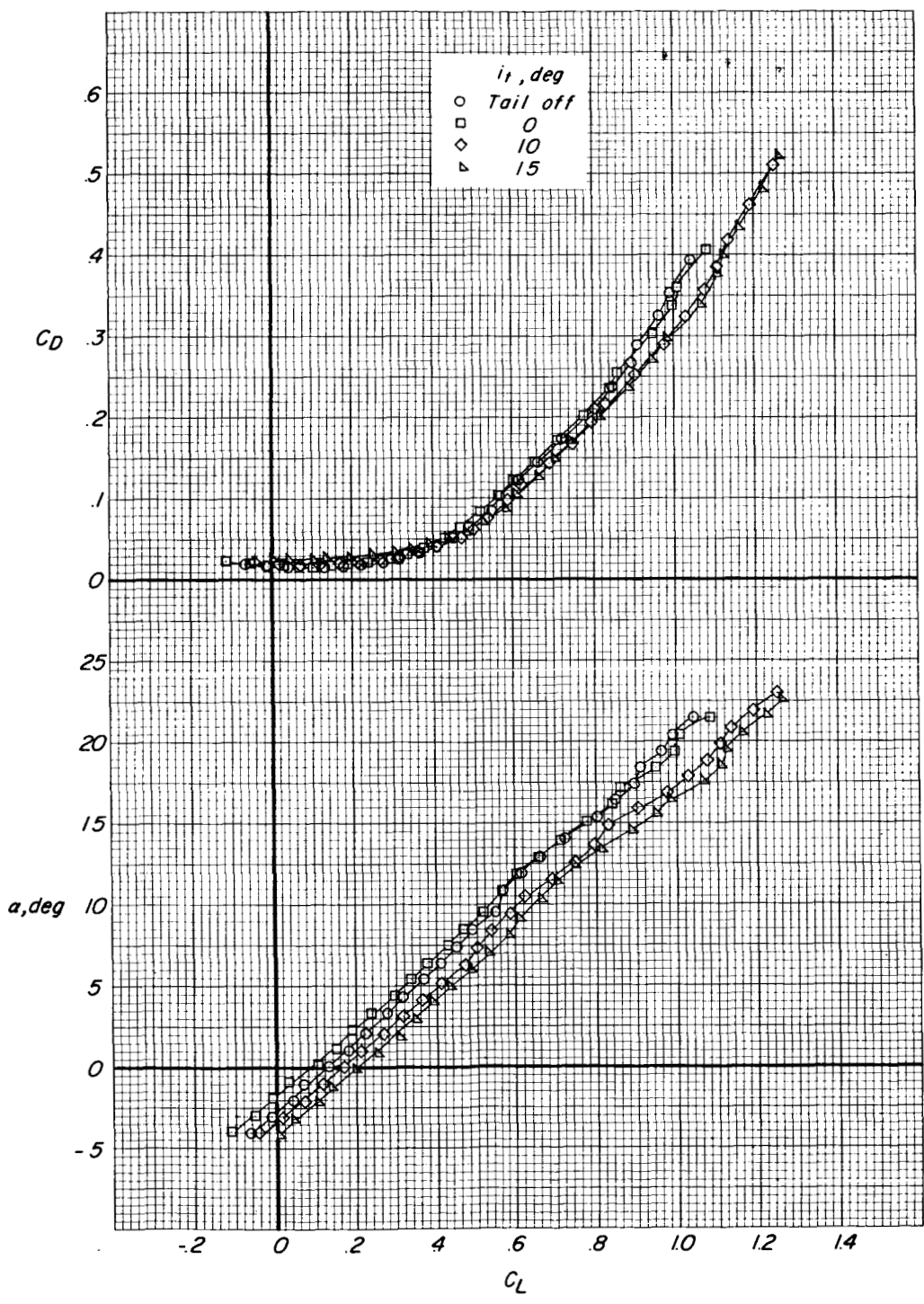


Figure 5.- Aerodynamic characteristics in pitch of the basic model configuration with the wing swept back 25°.

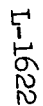


Figure 5.- Continued.

[REDACTED]

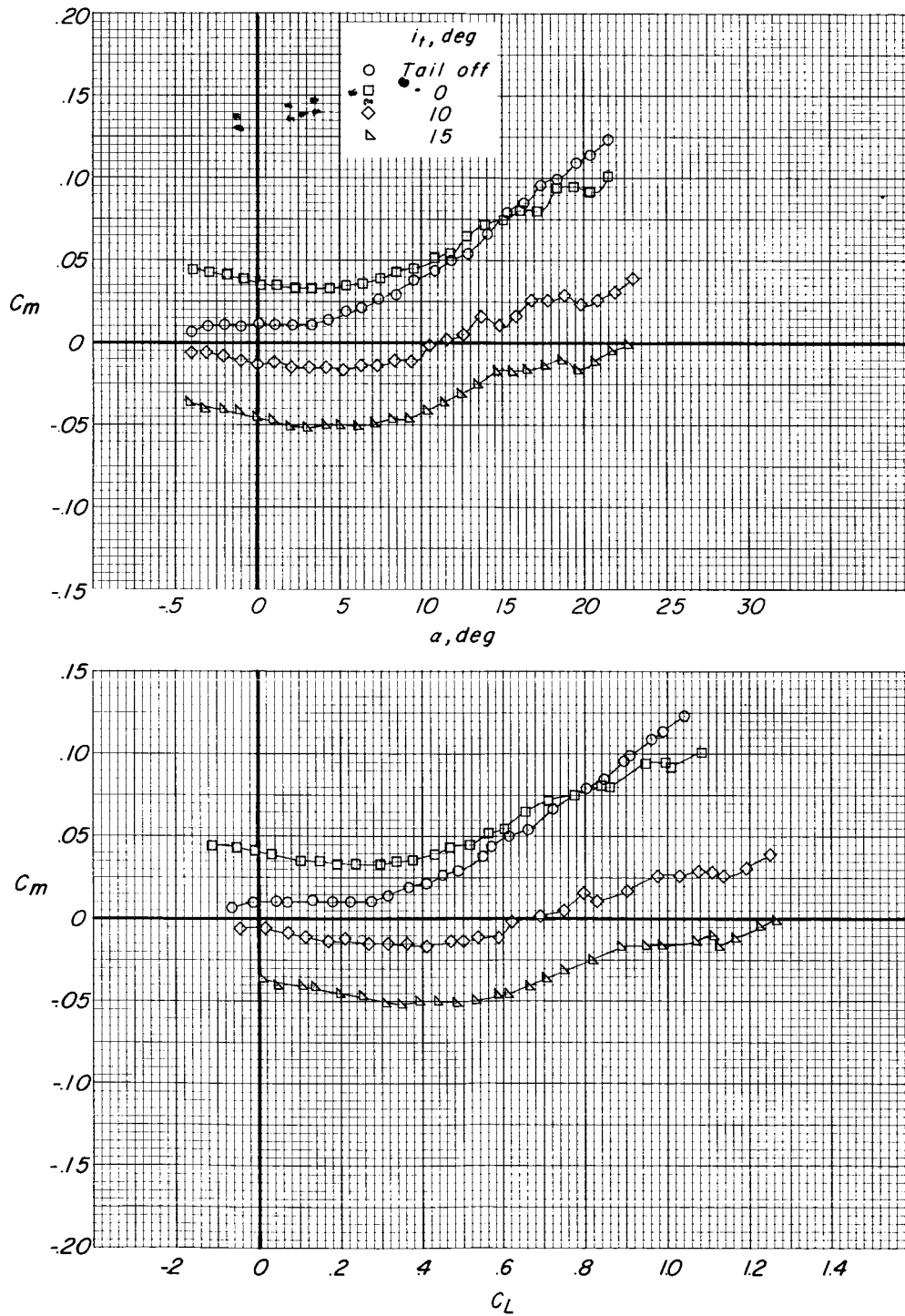
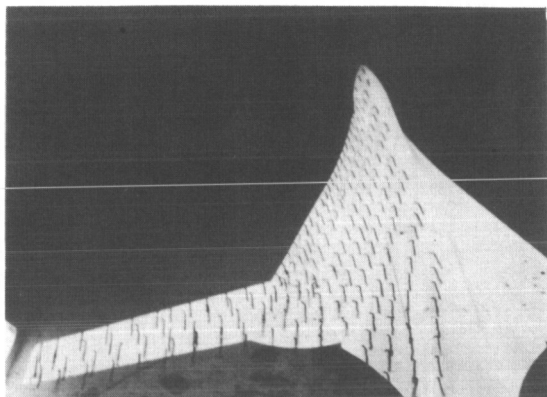
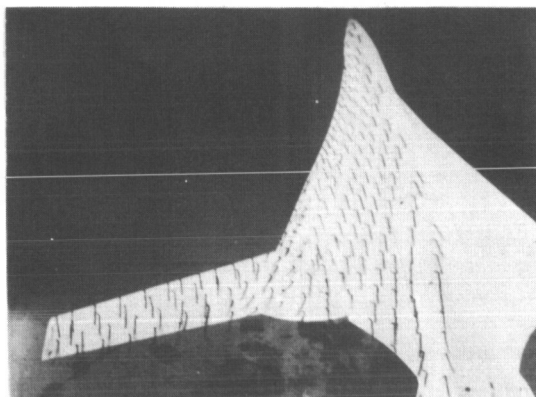
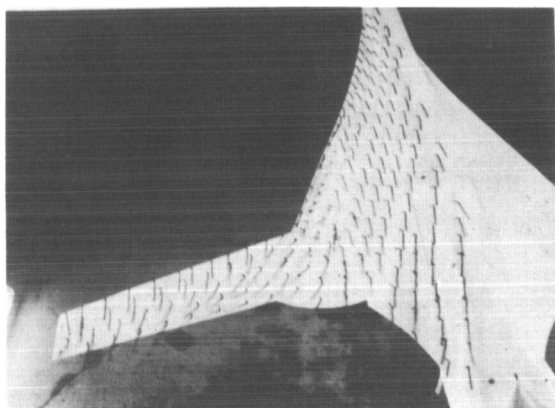
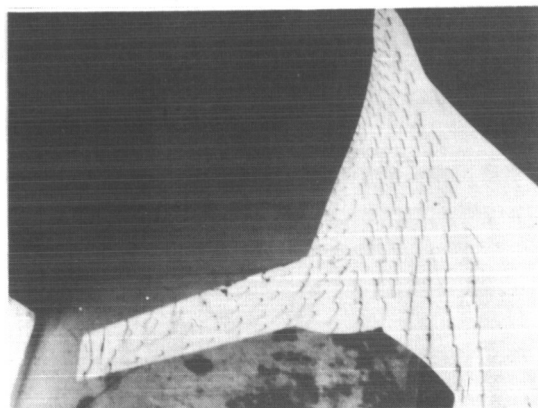


Figure 5.- Concluded.

0374-1-1034

 $\alpha = .10^\circ$  $\alpha = 4.33^\circ$  $\alpha = 6.38^\circ$  $\alpha = 8.51^\circ$

L-61-5118

Figure 6.- Flow over the surface of the basic model configuration as indicated by woolen tufts.

CONFIDENTIAL

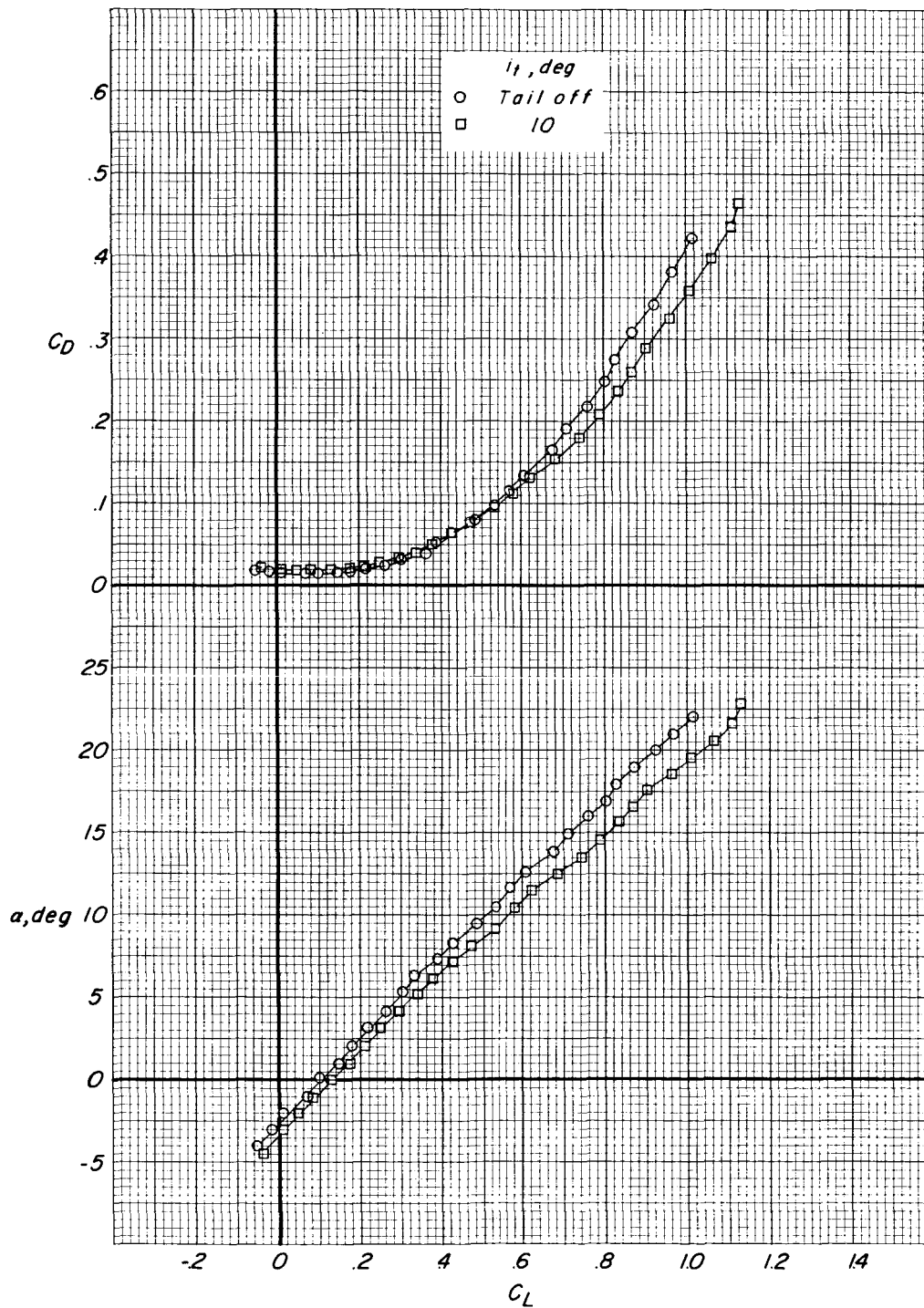


Figure 7.- Aerodynamic characteristics in pitch of the basic model configuration with the wing swept back 45° .

SECRET

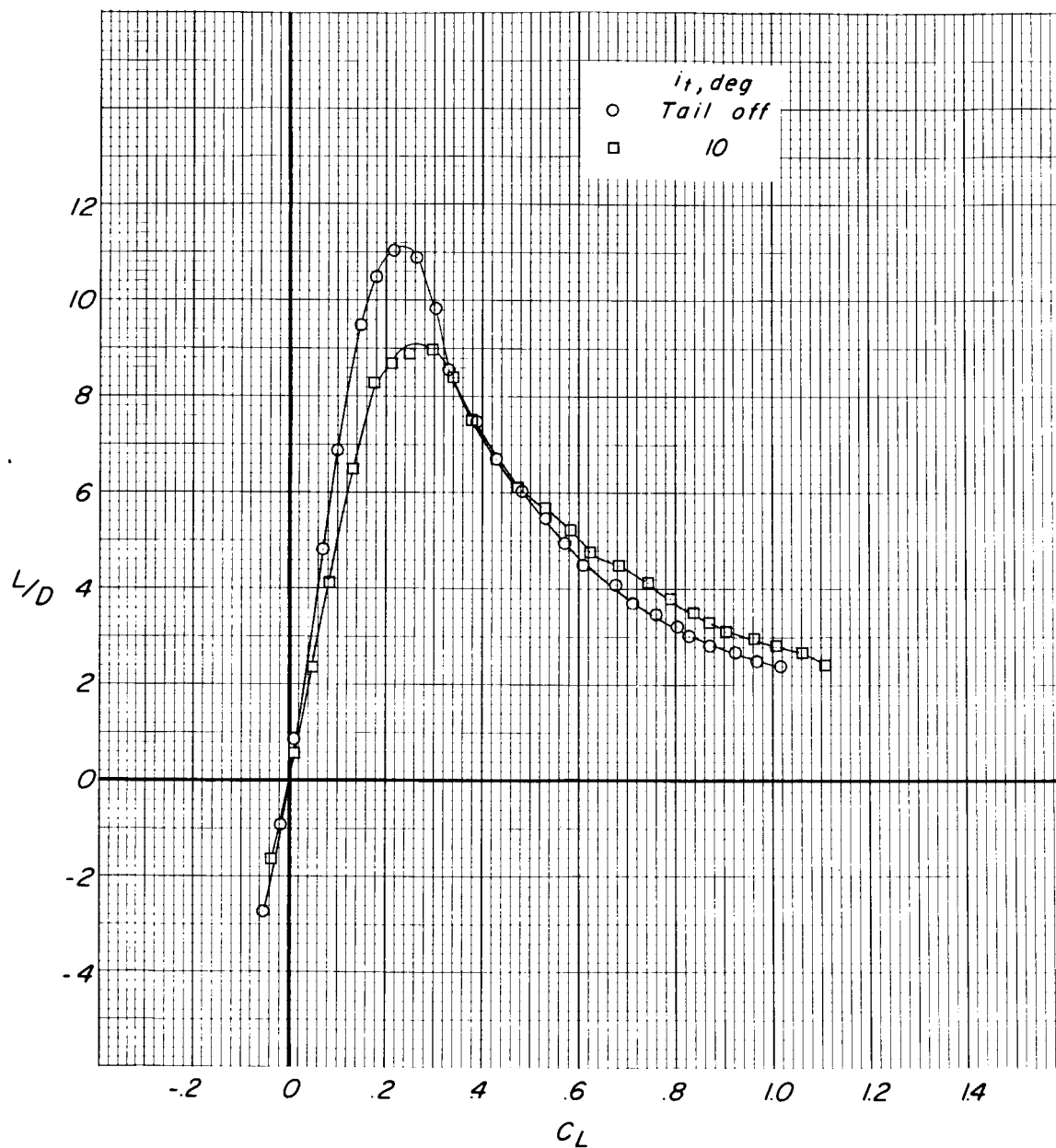


Figure 7.- Continued.

DECLASSIFIED

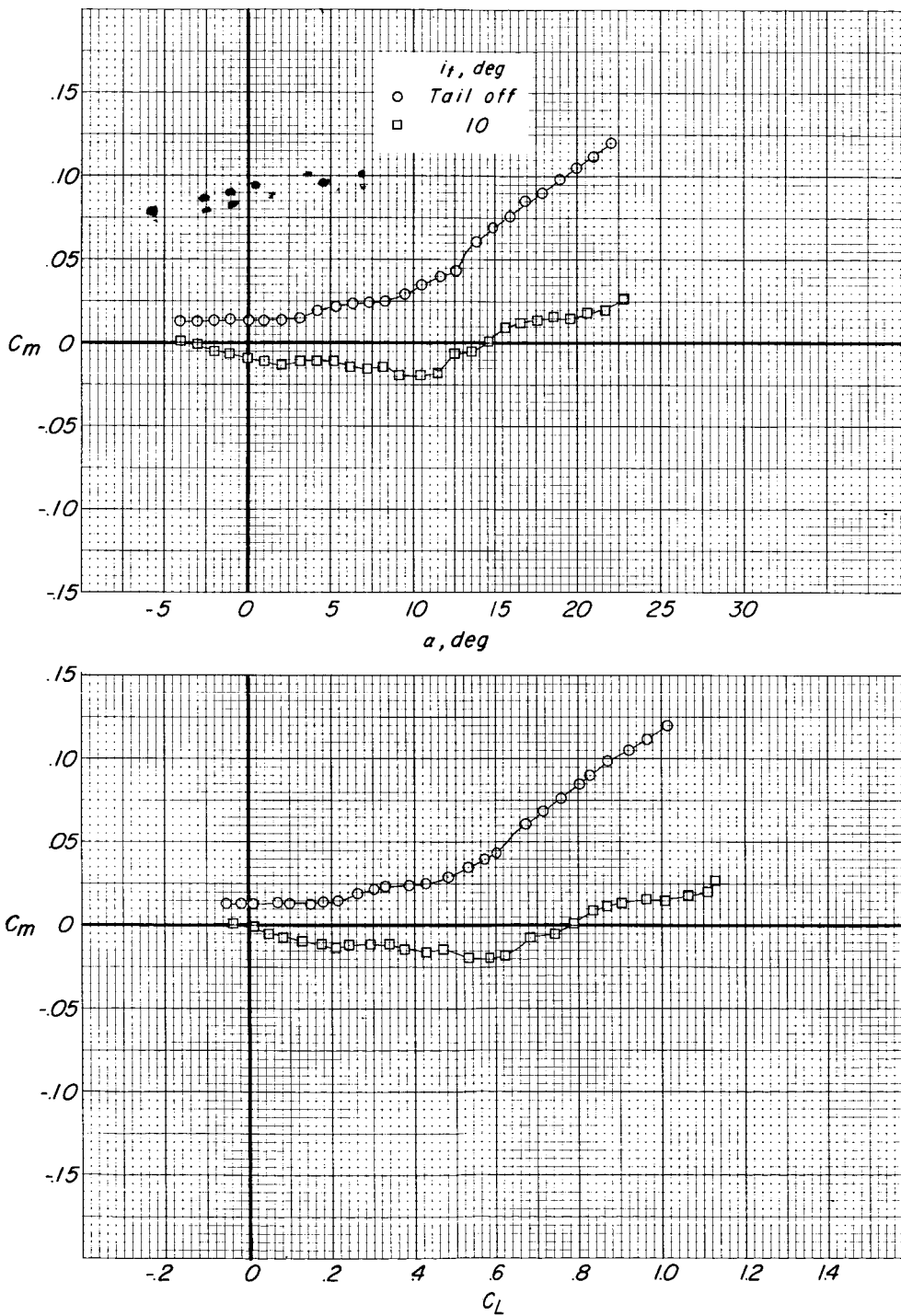


Figure 7.- Concluded.

CONFIDENTIAL

031711-1030

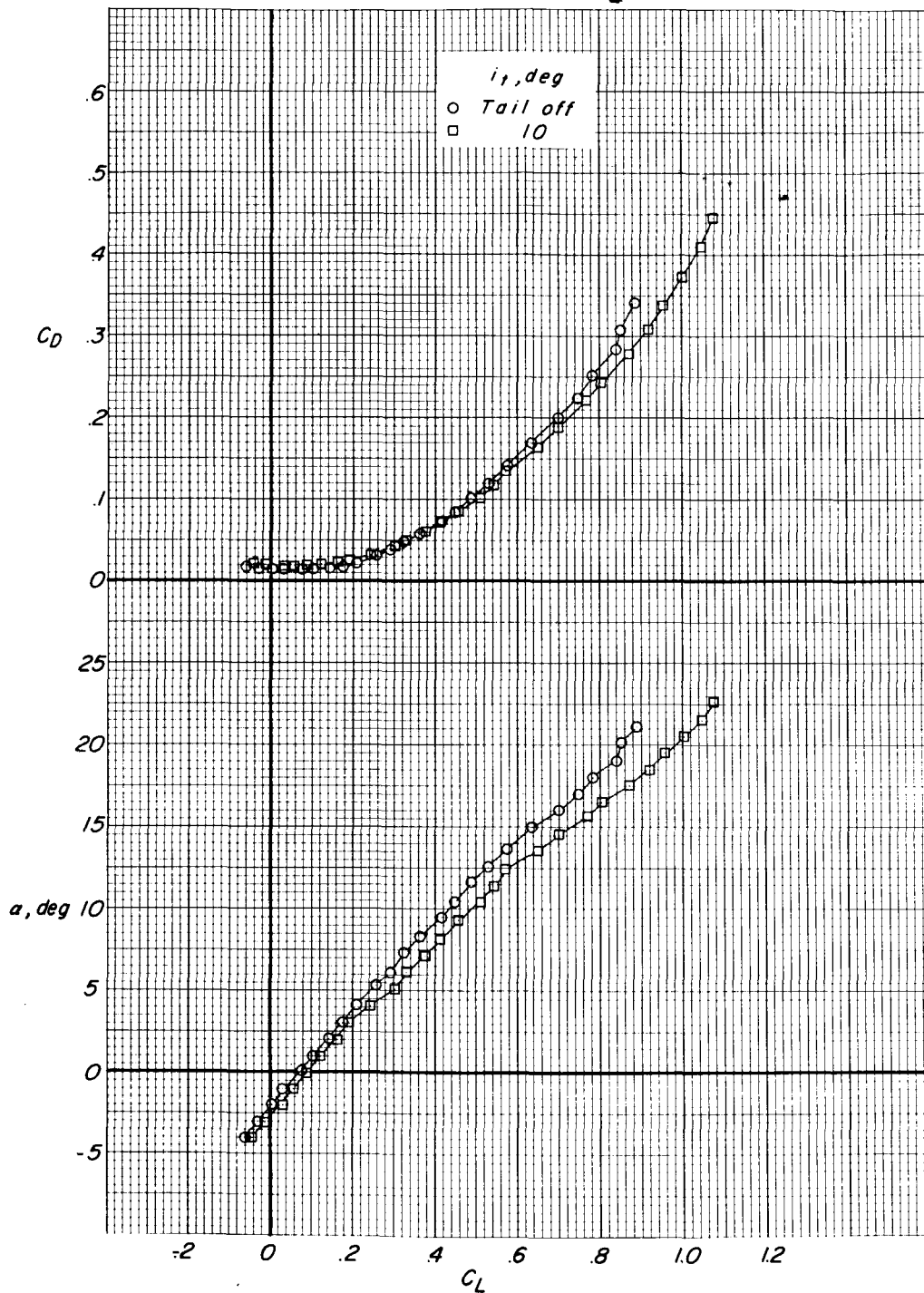


Figure 8.- Aerodynamic characteristics in pitch of the basic model configuration with the wing swept back 60° .

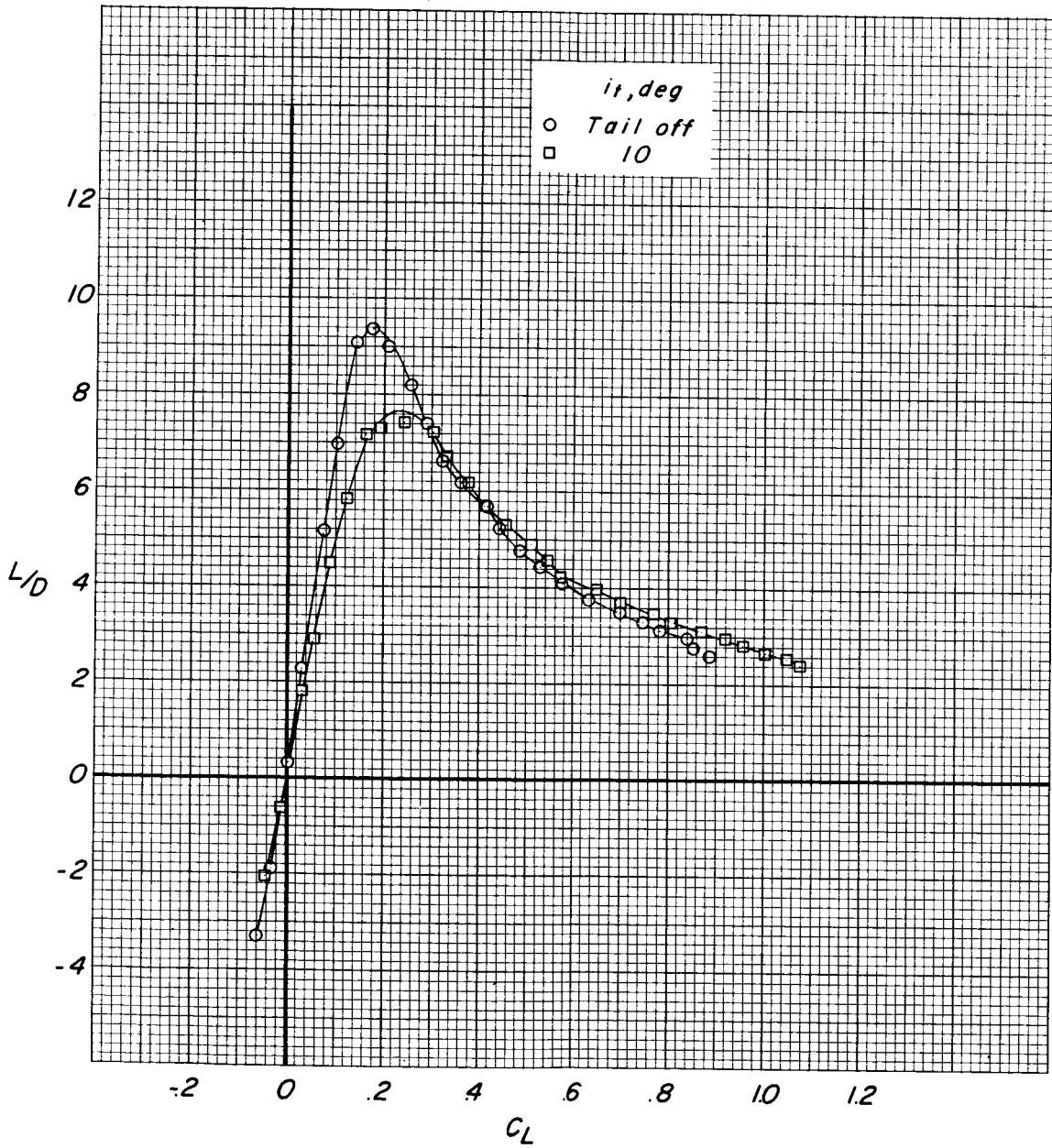


Figure 8.- Continued.

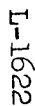


Figure 8.- Concluded.

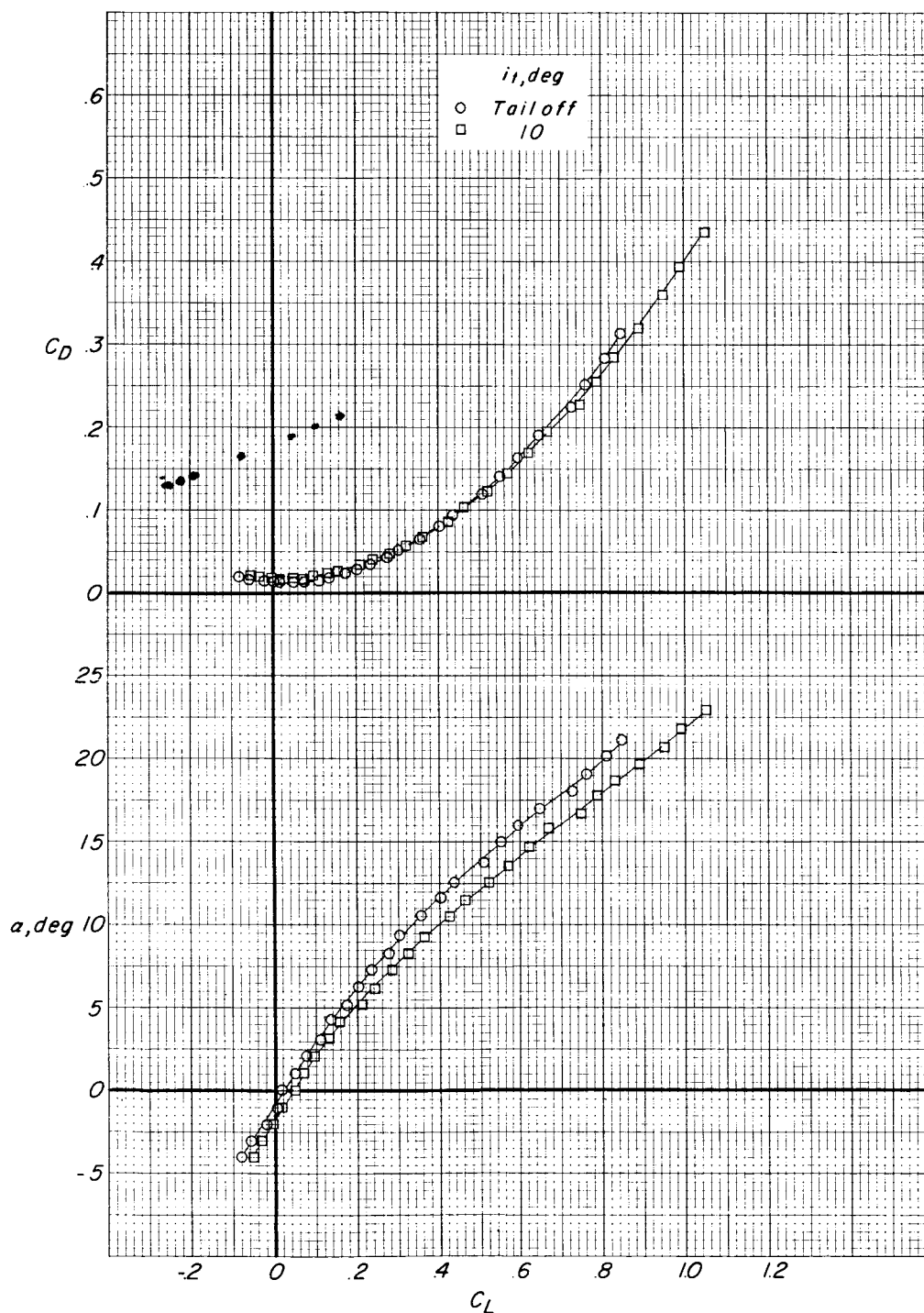


Figure 9.- Aerodynamic characteristics in pitch of the basic model configuration with the wing swept back 80°.

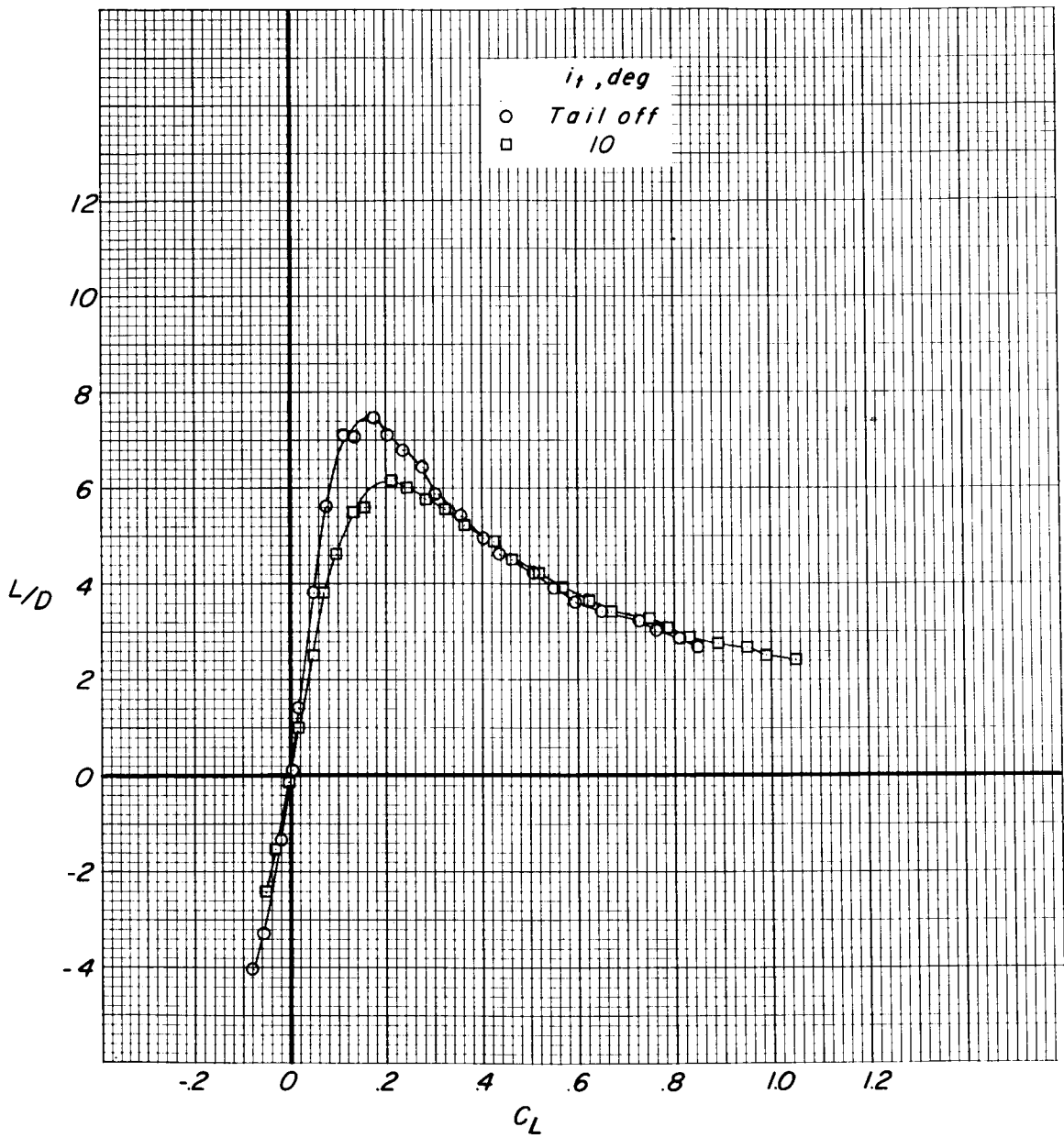


Figure 9.- Continued.

DECLASSIFIED

L-1622

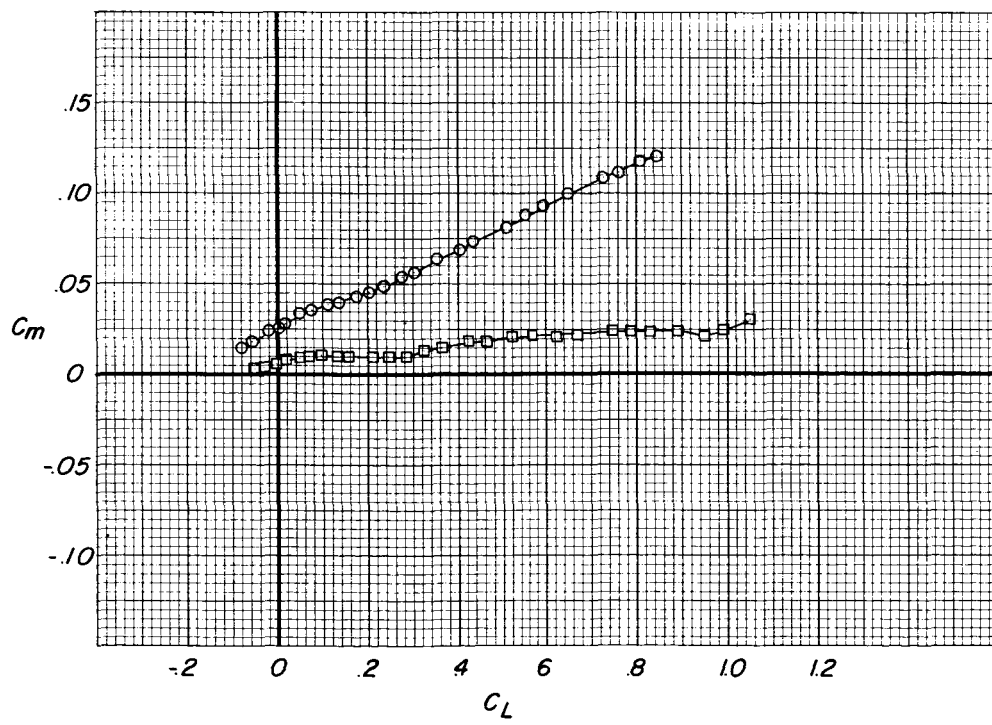
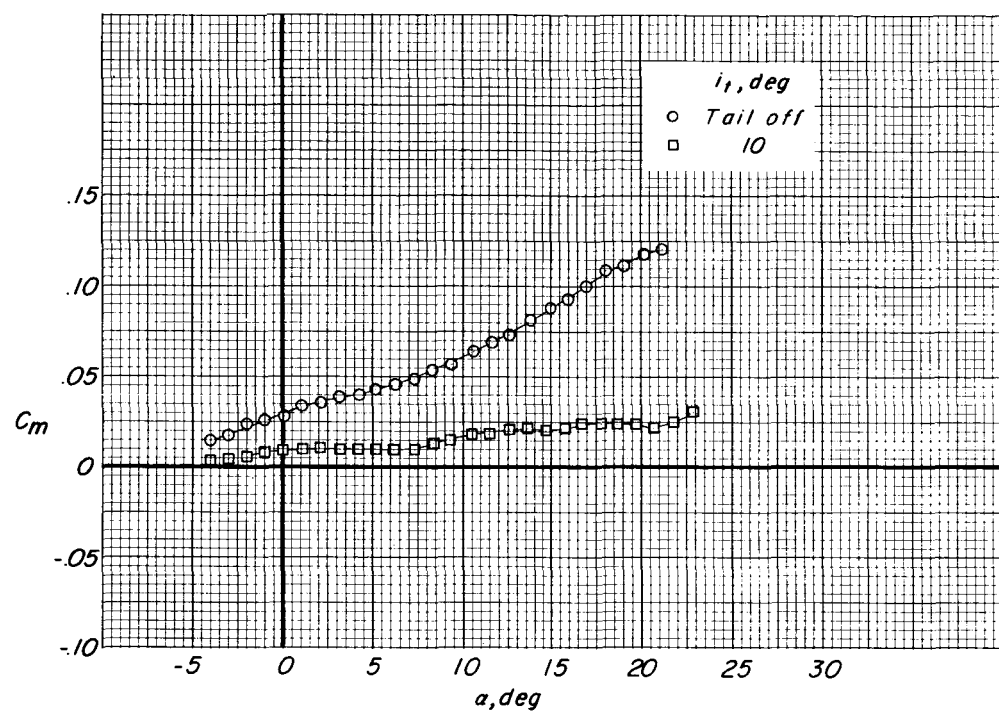


Figure 9.- Concluded.

DECLASSIFIED

0375 1030

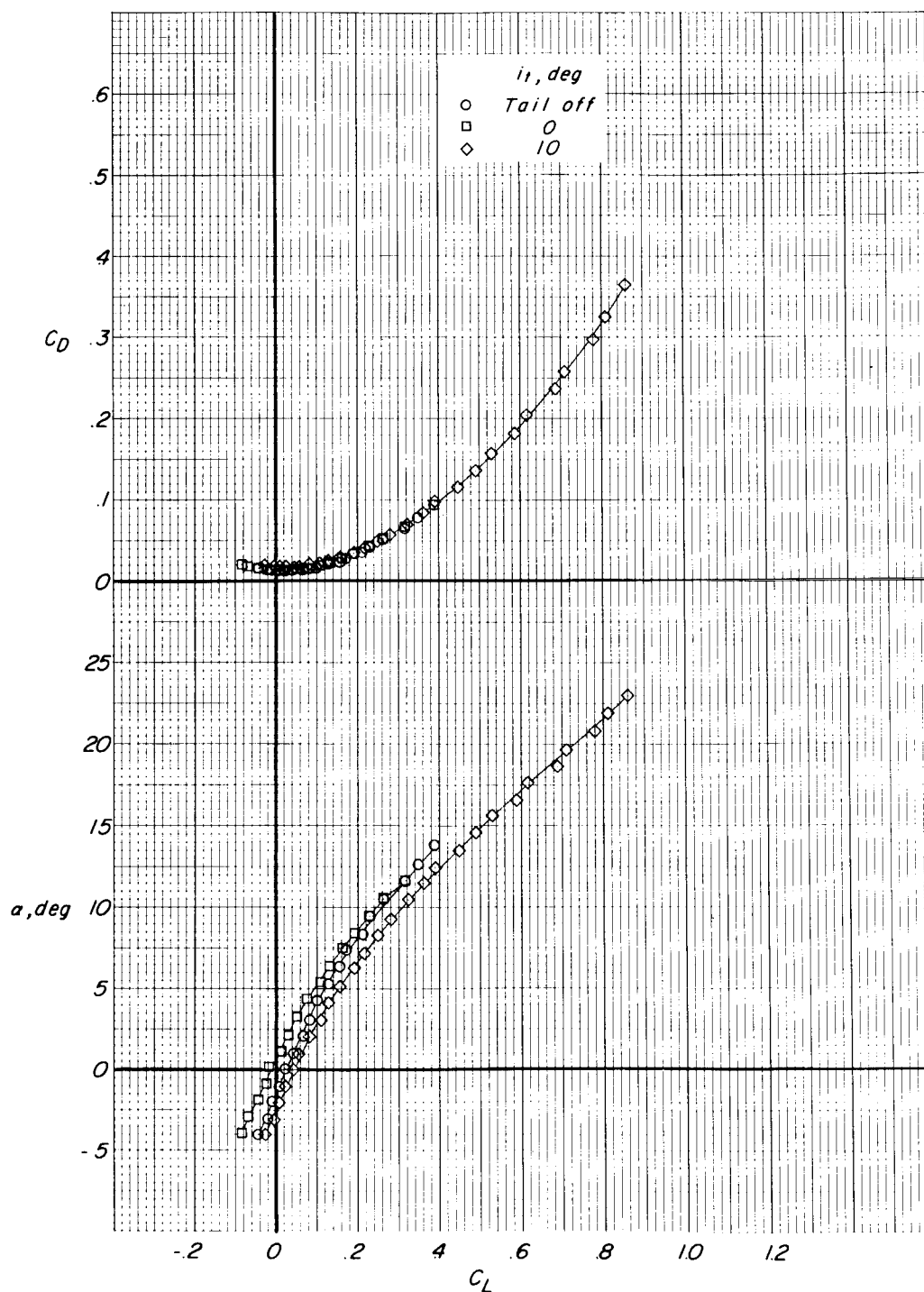


Figure 10.- Aerodynamic characteristics in pitch of the basic model configuration with the wing outer panels removed.

DECLASSIFIED

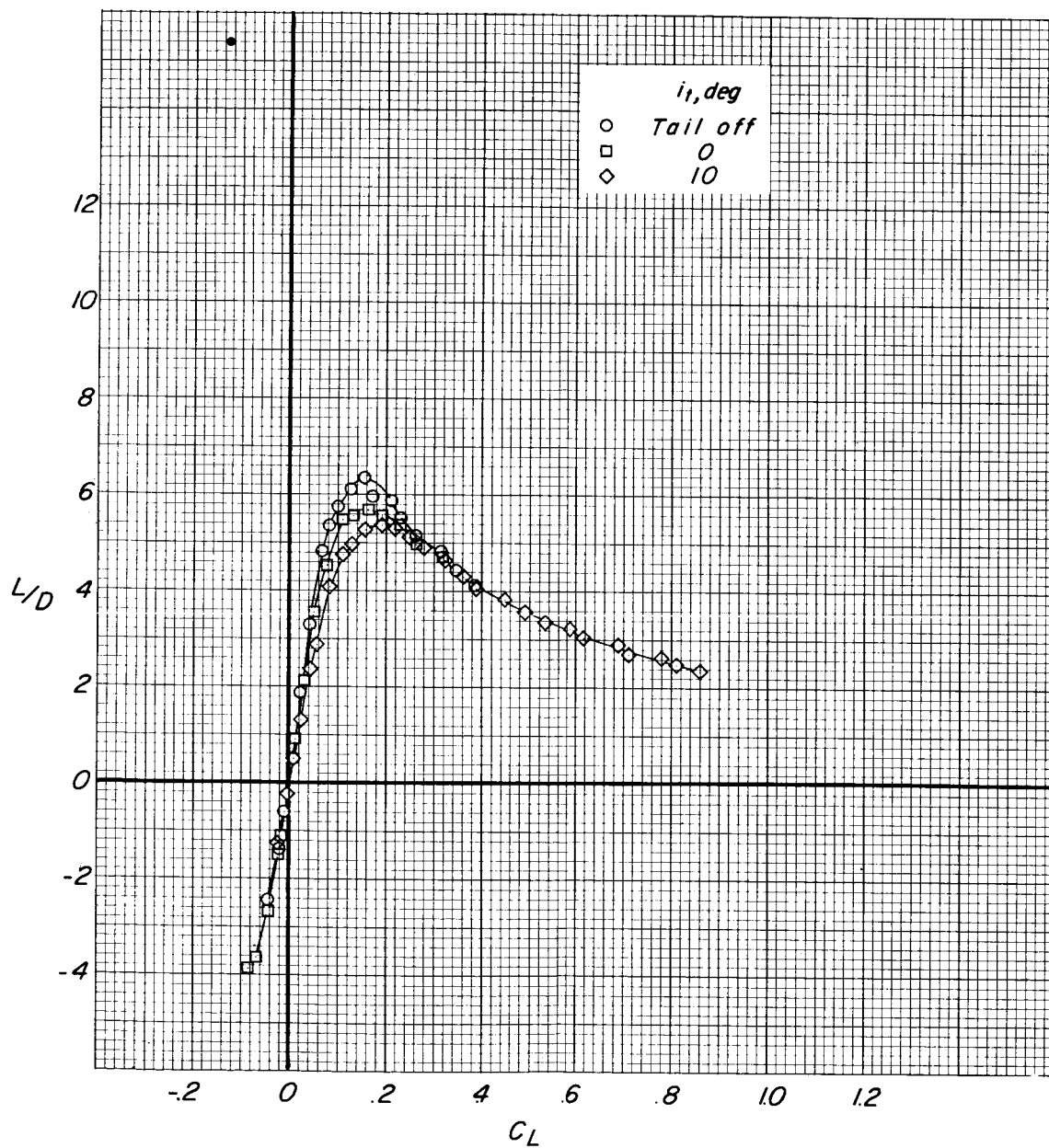


Figure 10.- Continued.

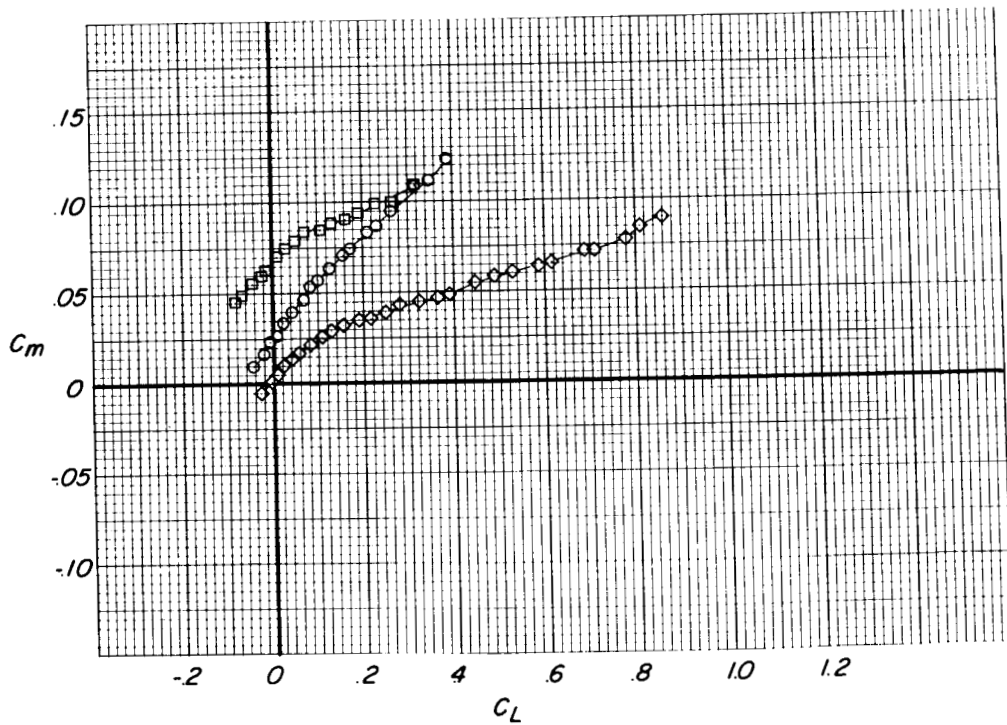
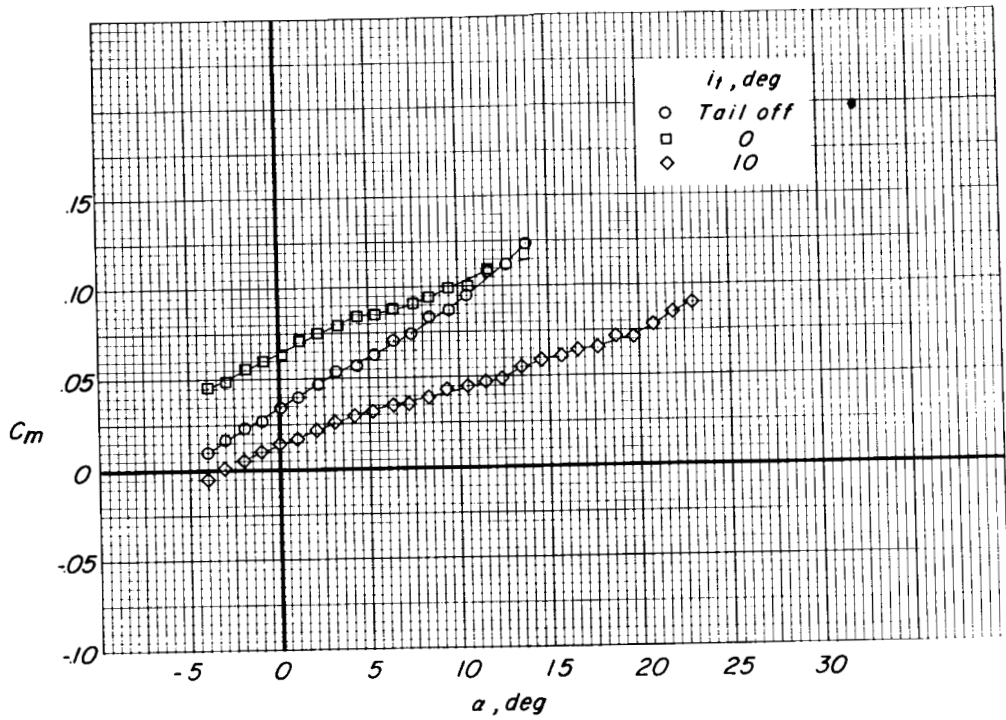


Figure 10.- Concluded.

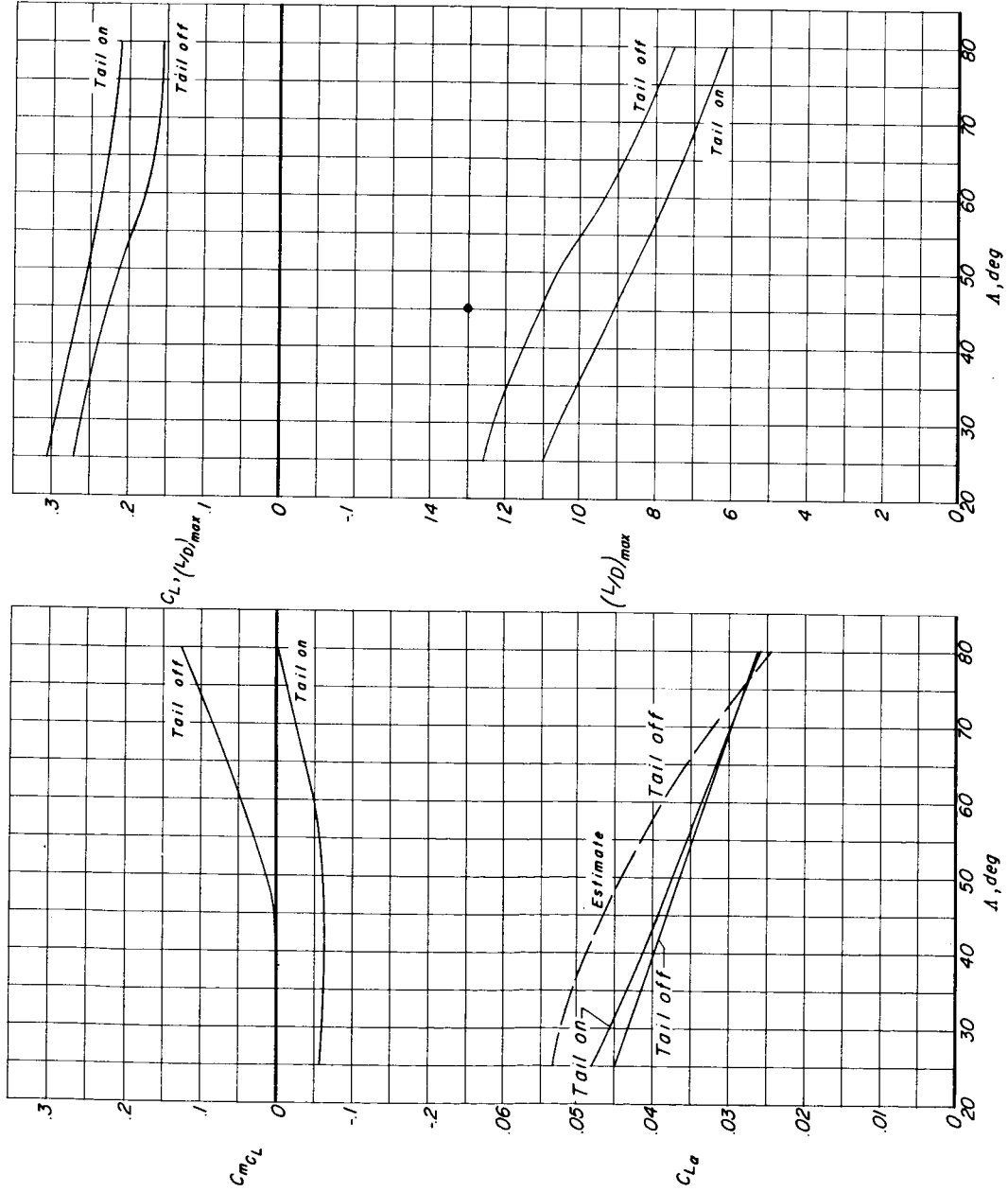


Figure 11.- Summary of effects of wing sweep on stability and performance parameters of the basic model configuration.

031754.1030

I-1622

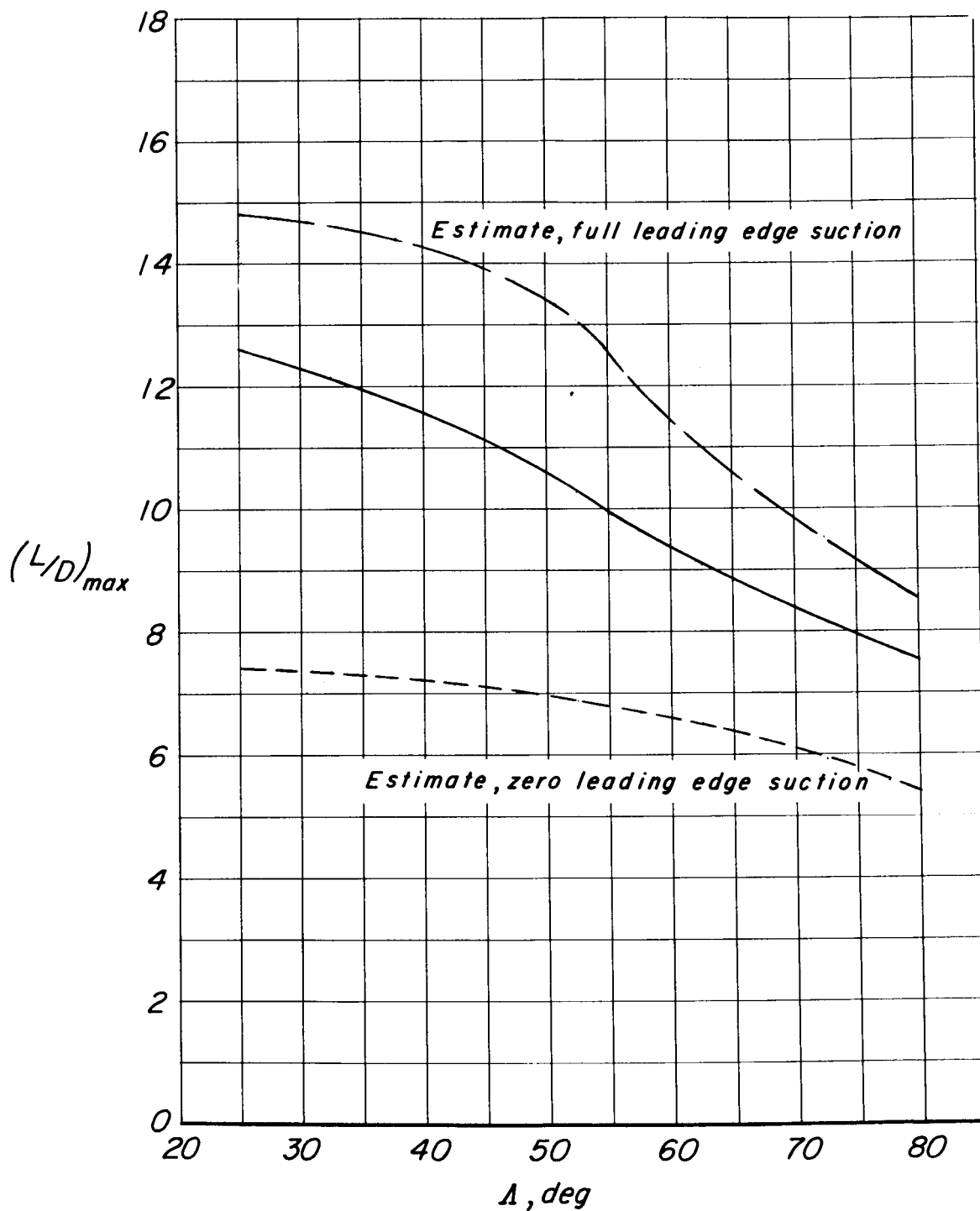


Figure 11.- Concluded.

Δ, deg
25
45
60
80

OUT 4

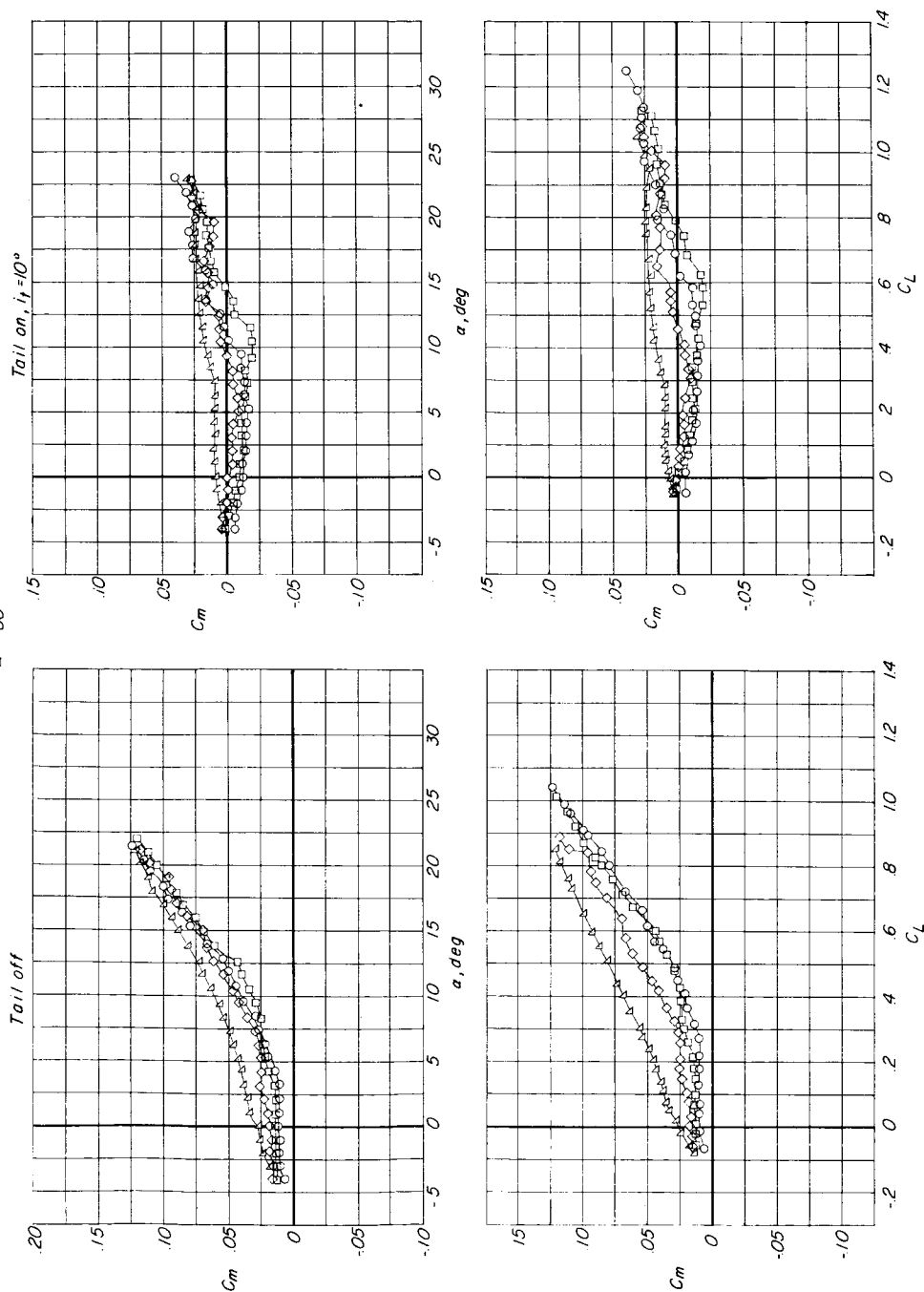


Figure 12.- Effects of wing sweep on pitching moments of the basic model configuration.

CONFIDENTIAL

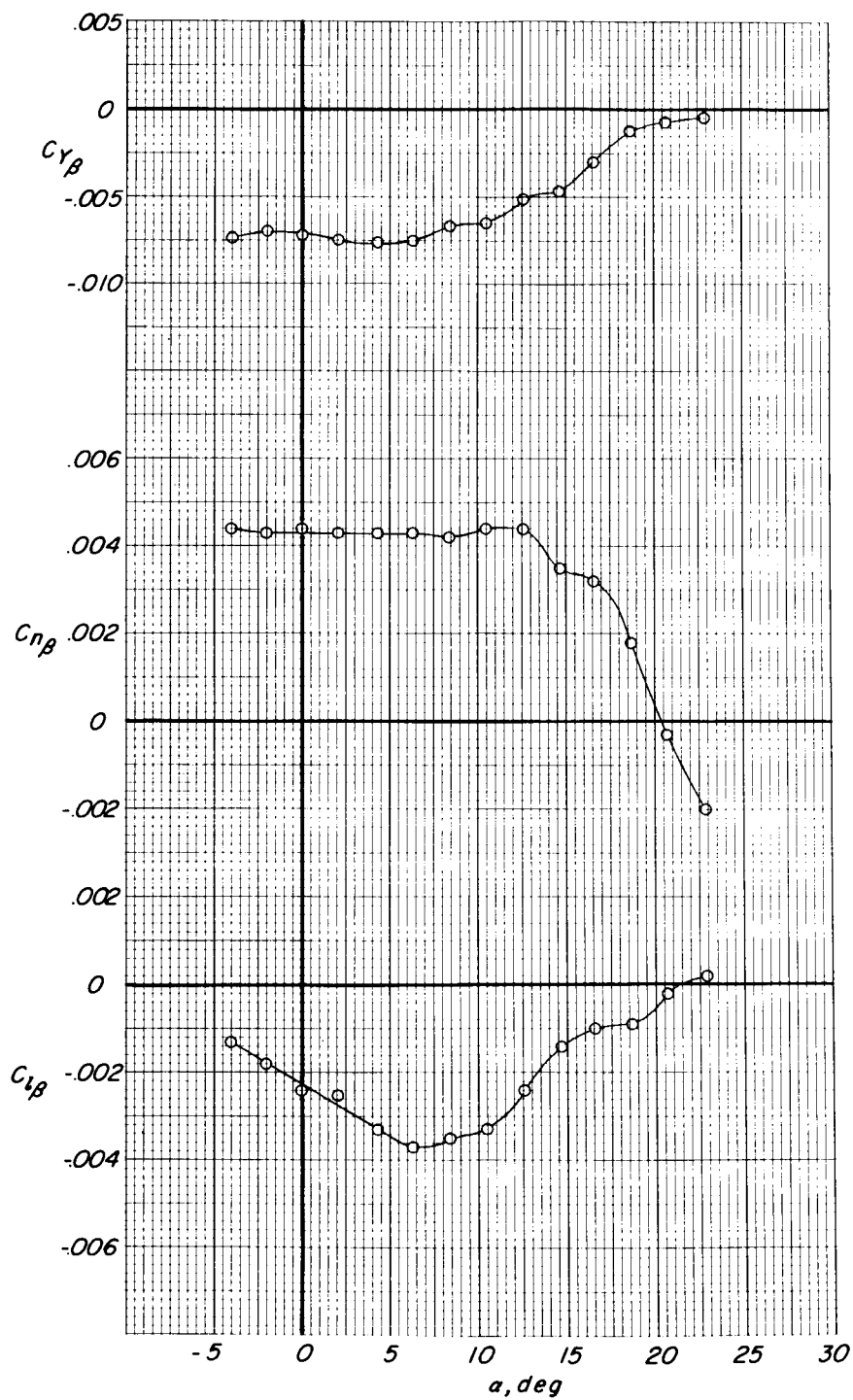


Figure 13.- Lateral stability derivatives of the basic model configuration with the wing swept back 25° . $i_t = 10^\circ$.

CONFIDENTIAL

SECRET

45

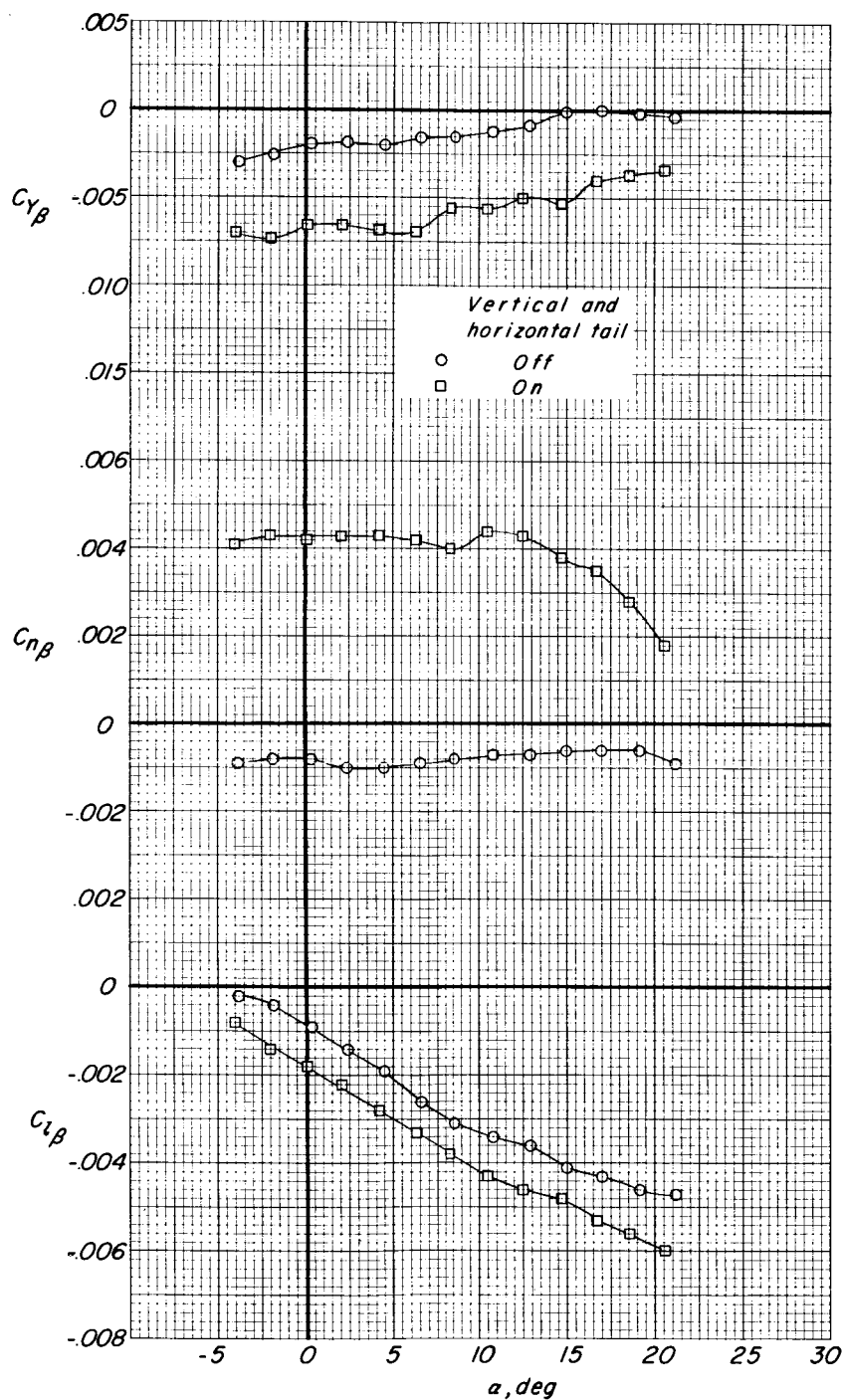


Figure 14.- Lateral stability derivatives of the basic model configuration with the wing swept back 80° . $i_t = 10^\circ$ with horizontal tail on.

03 7 10 30

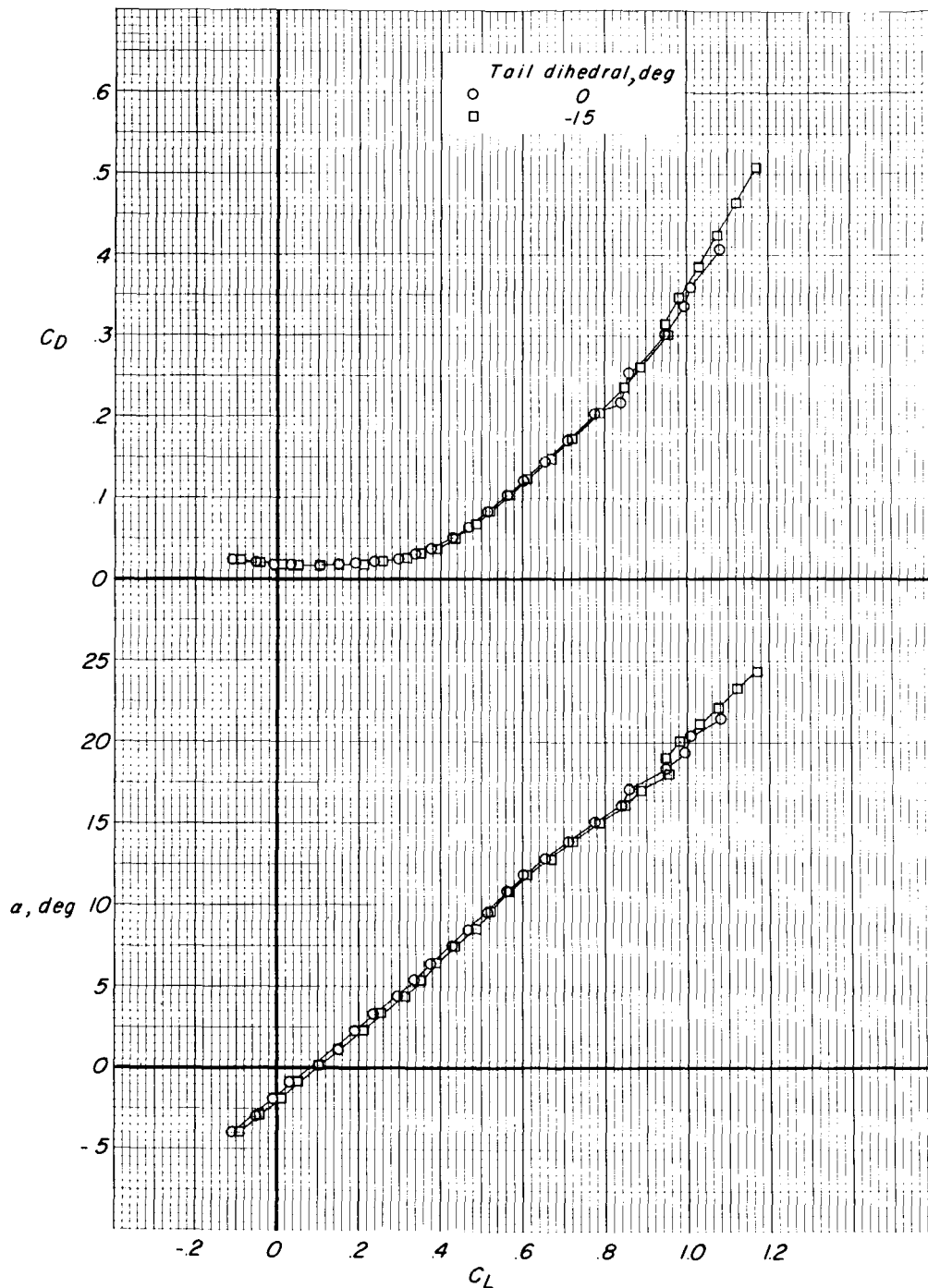


Figure 15.- Effect of -15° dihedral of the horizontal tail on the aerodynamic characteristics in pitch of the basic model configuration. $i_t = 0^\circ$.

DECLASSIFIED

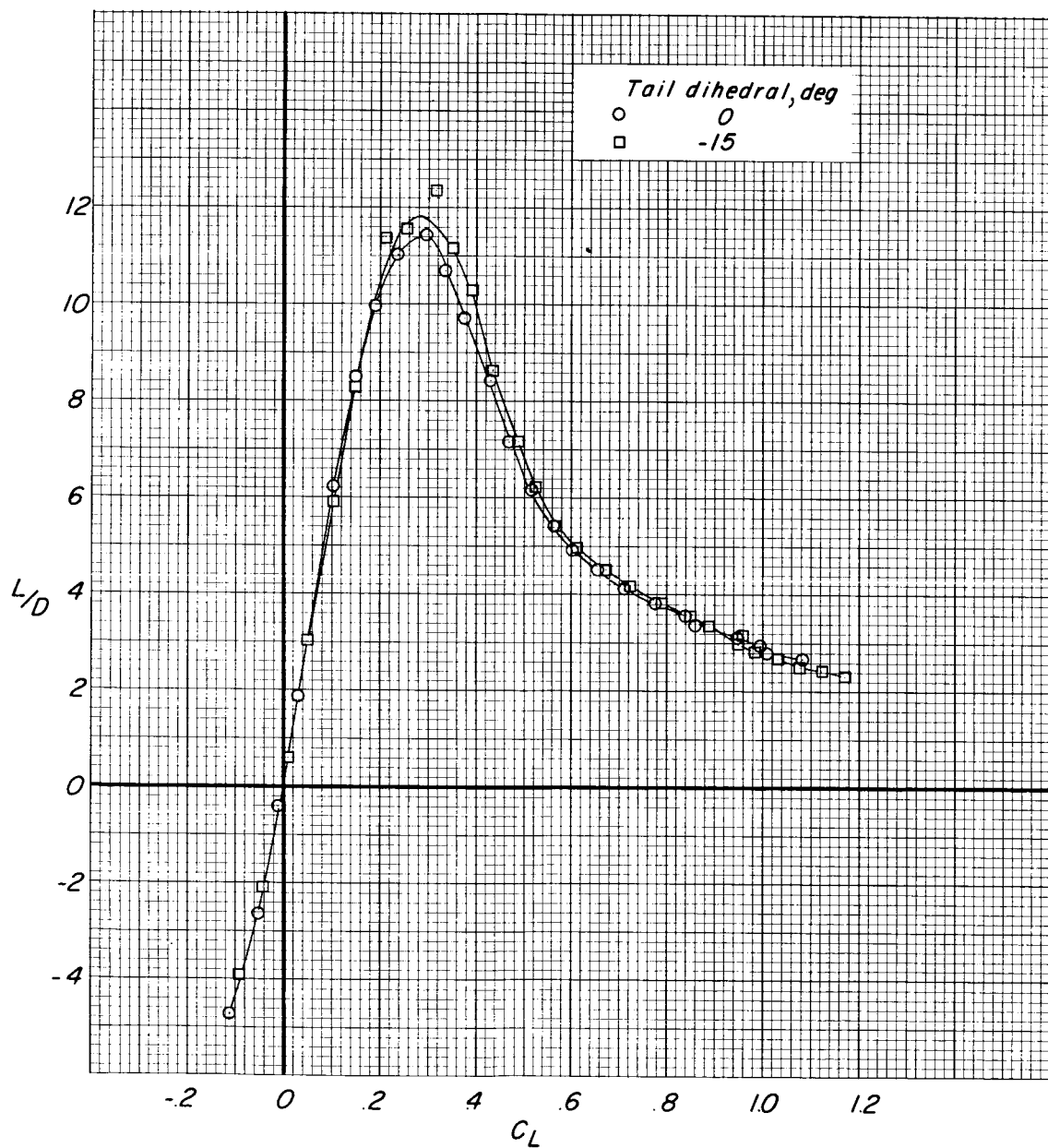


Figure 15.- Continued.

03 1030

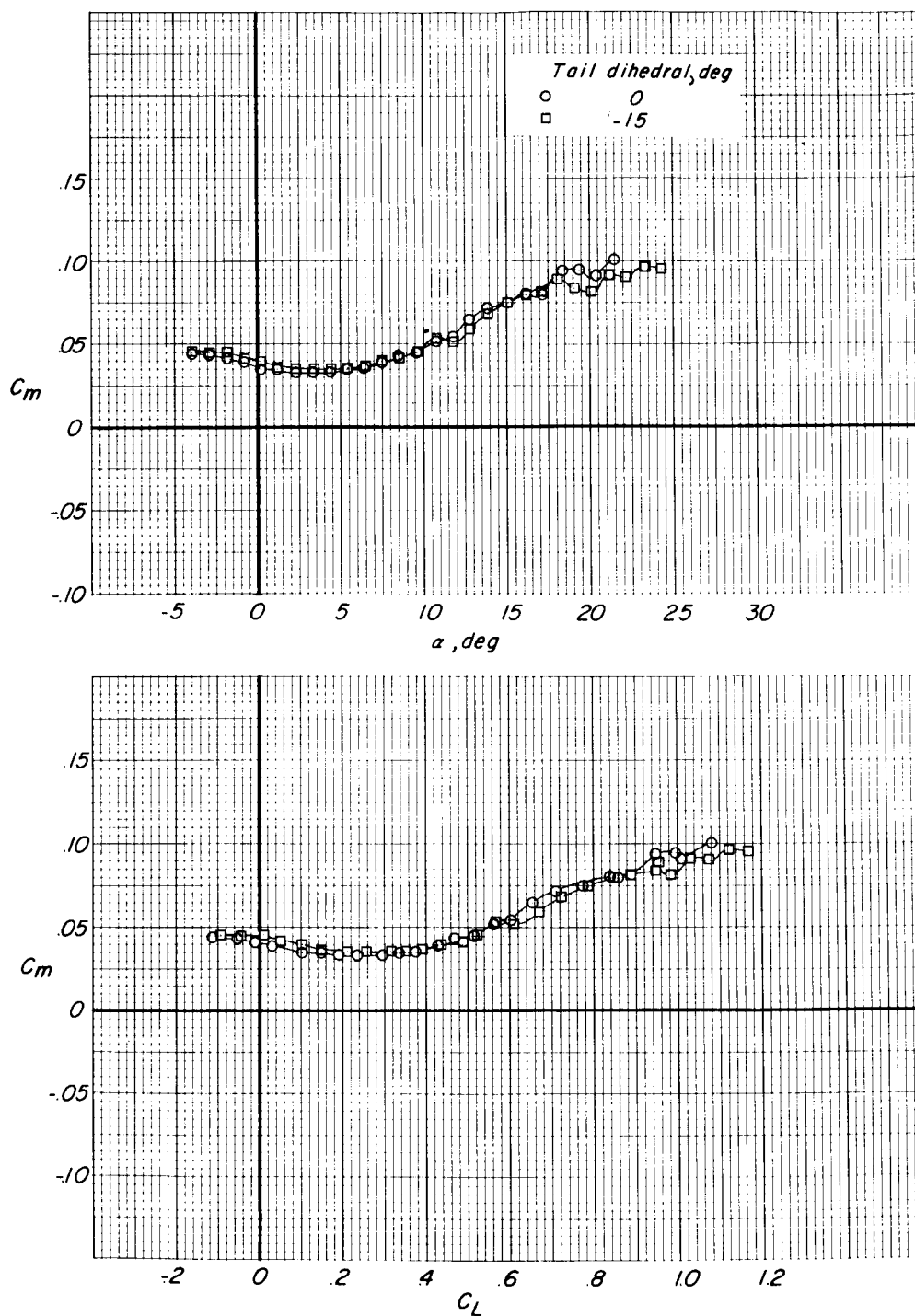


Figure 15.- Concluded.

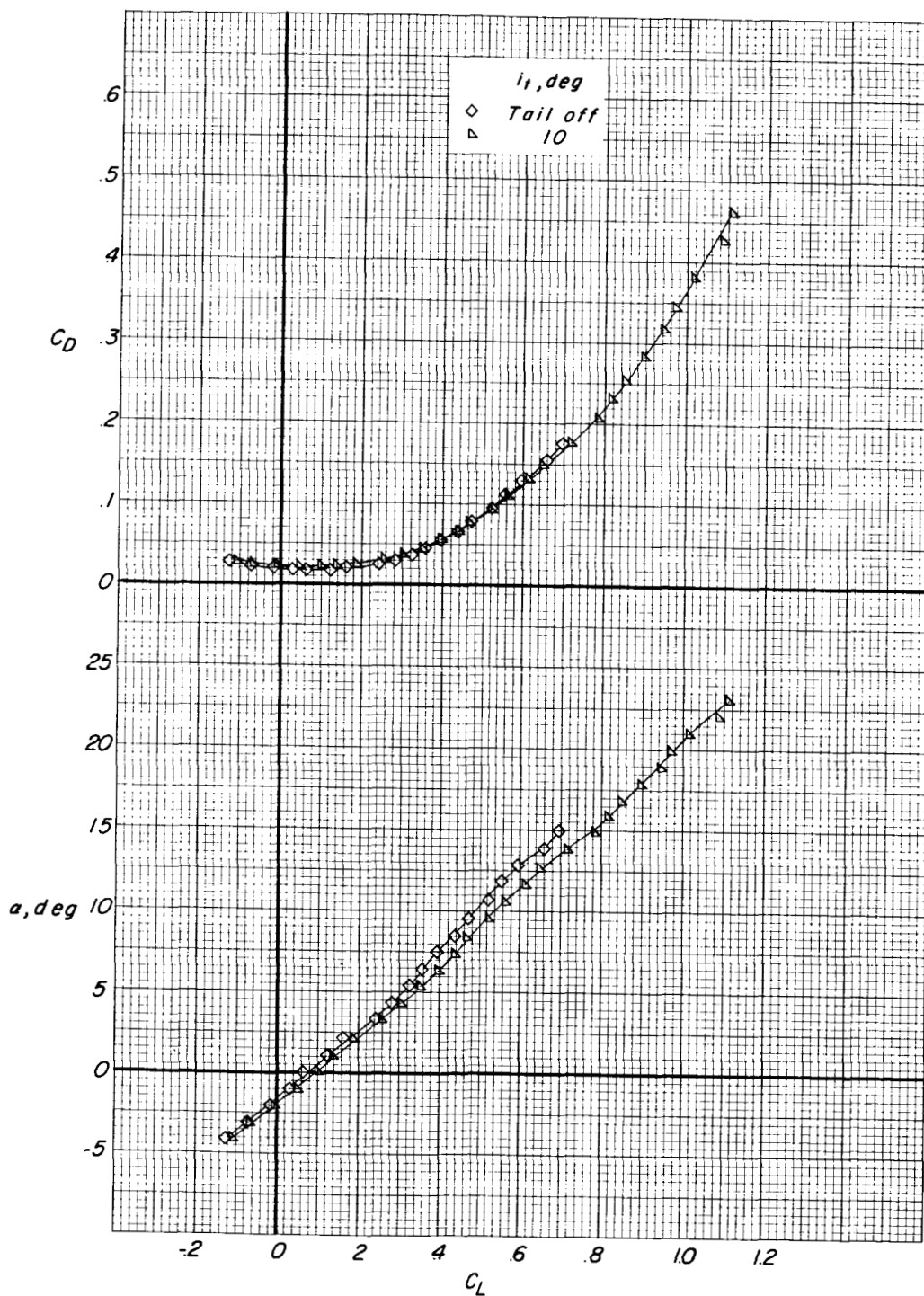


Figure 16.- Aerodynamic characteristics in pitch of the model with the wing outer panels moved forward with 25° of sweepback.

031324.030

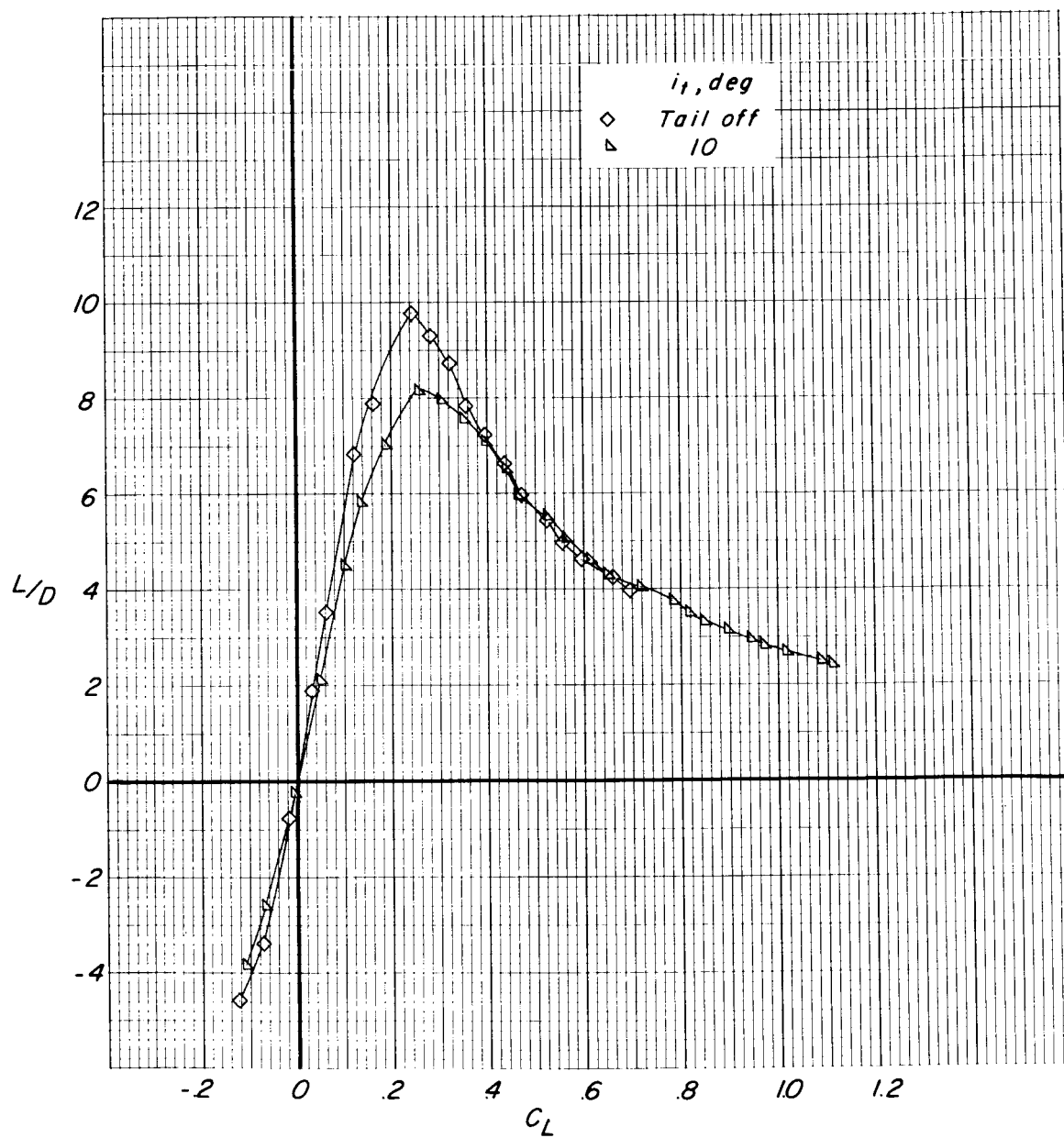


Figure 16.- Continued.

DECLASSIFIED

51

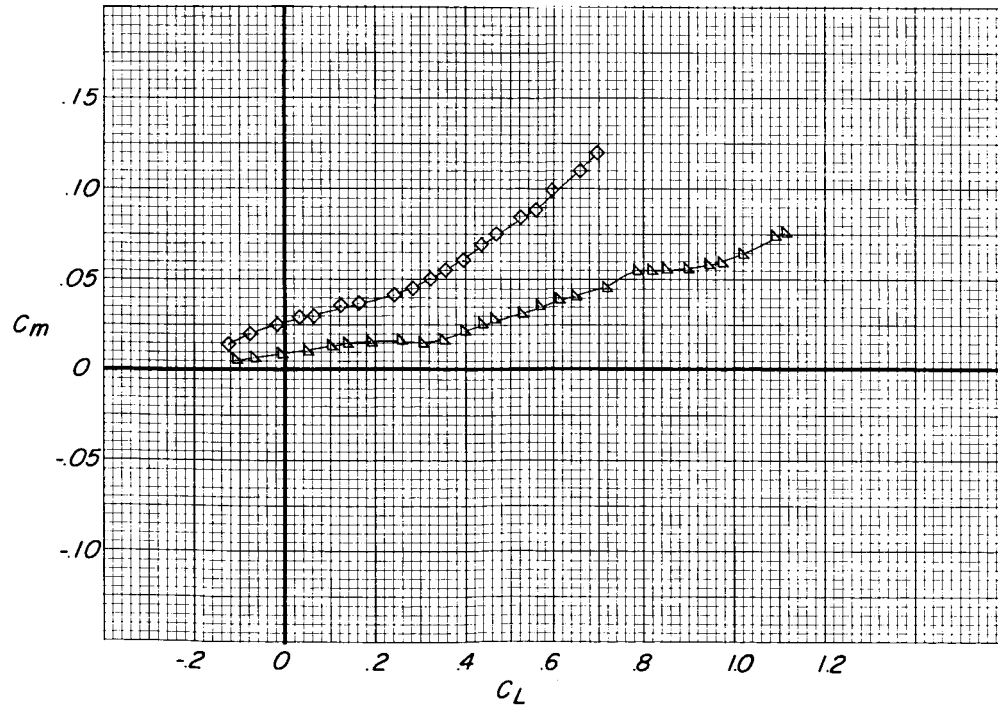
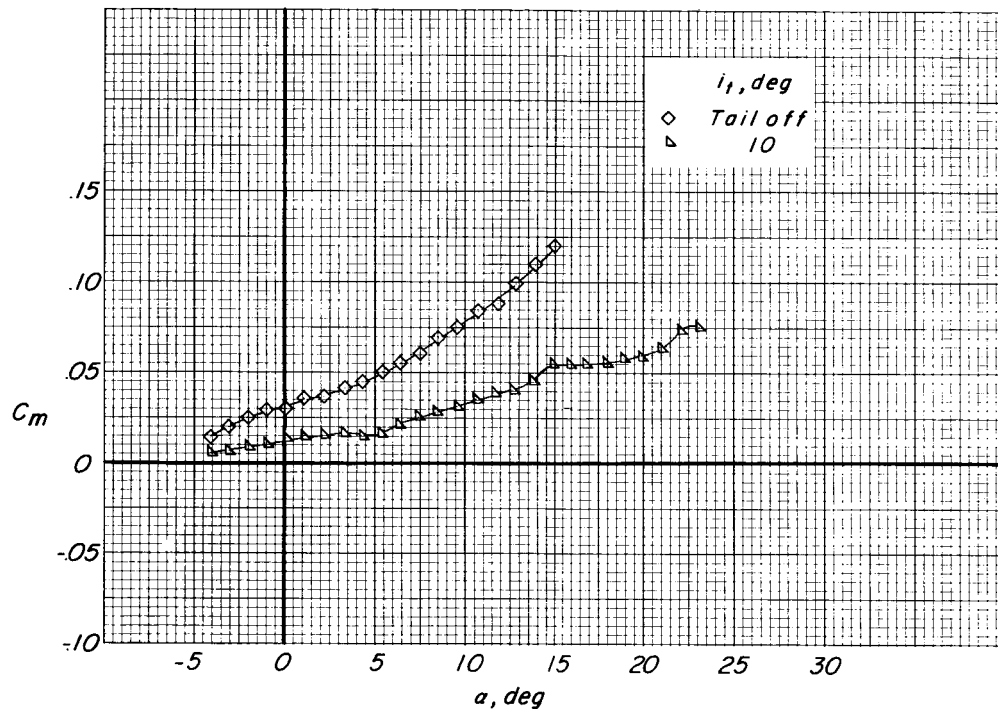


Figure 16.- Concluded.

031722-1030

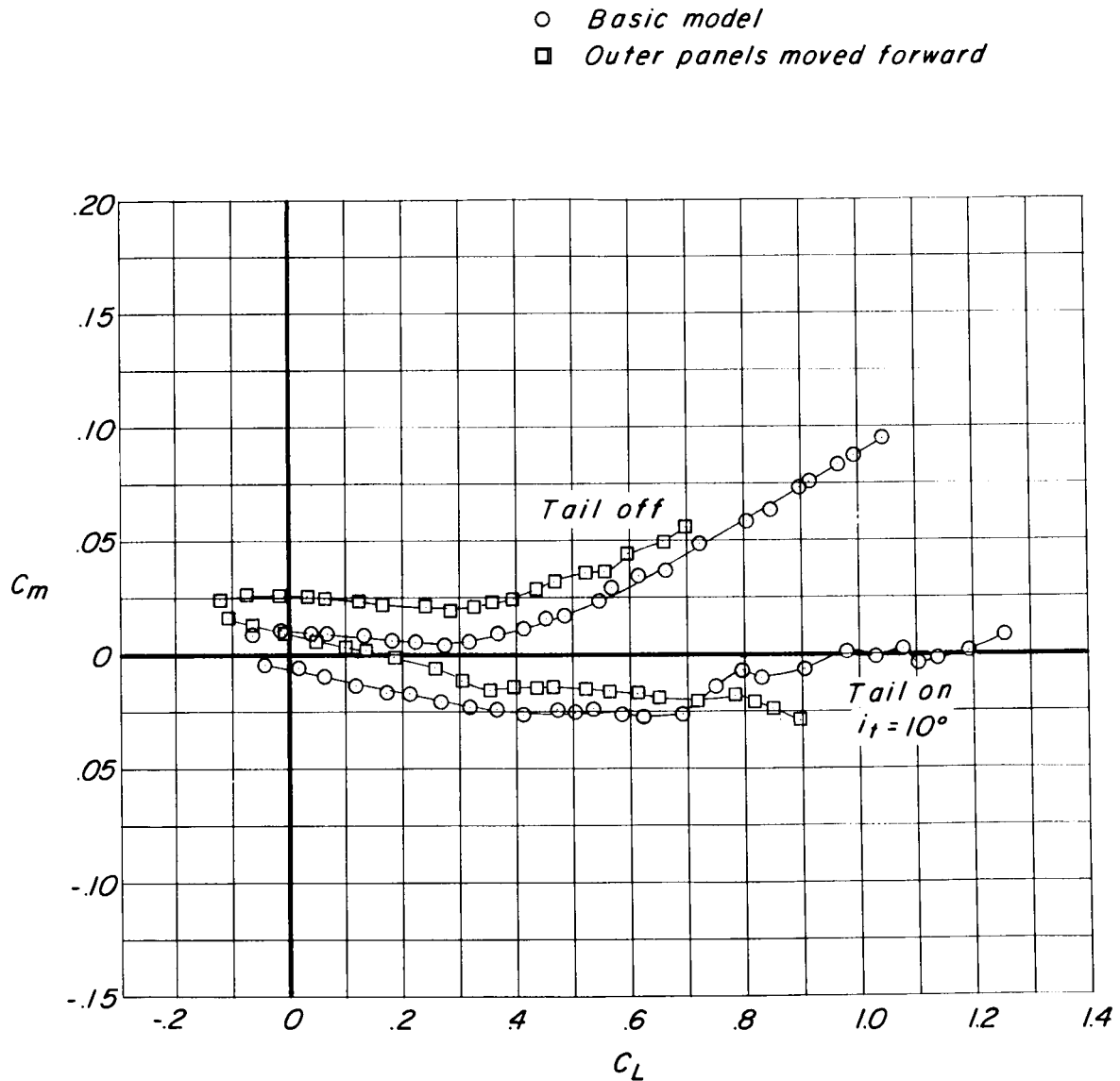


Figure 17.- Effect on pitching moments of moving the wing outer panels forward with $\Lambda = 25^\circ$. Moment reference shifted on both configurations to give approximately 5-percent static margin at low lift coefficients with the tail on.

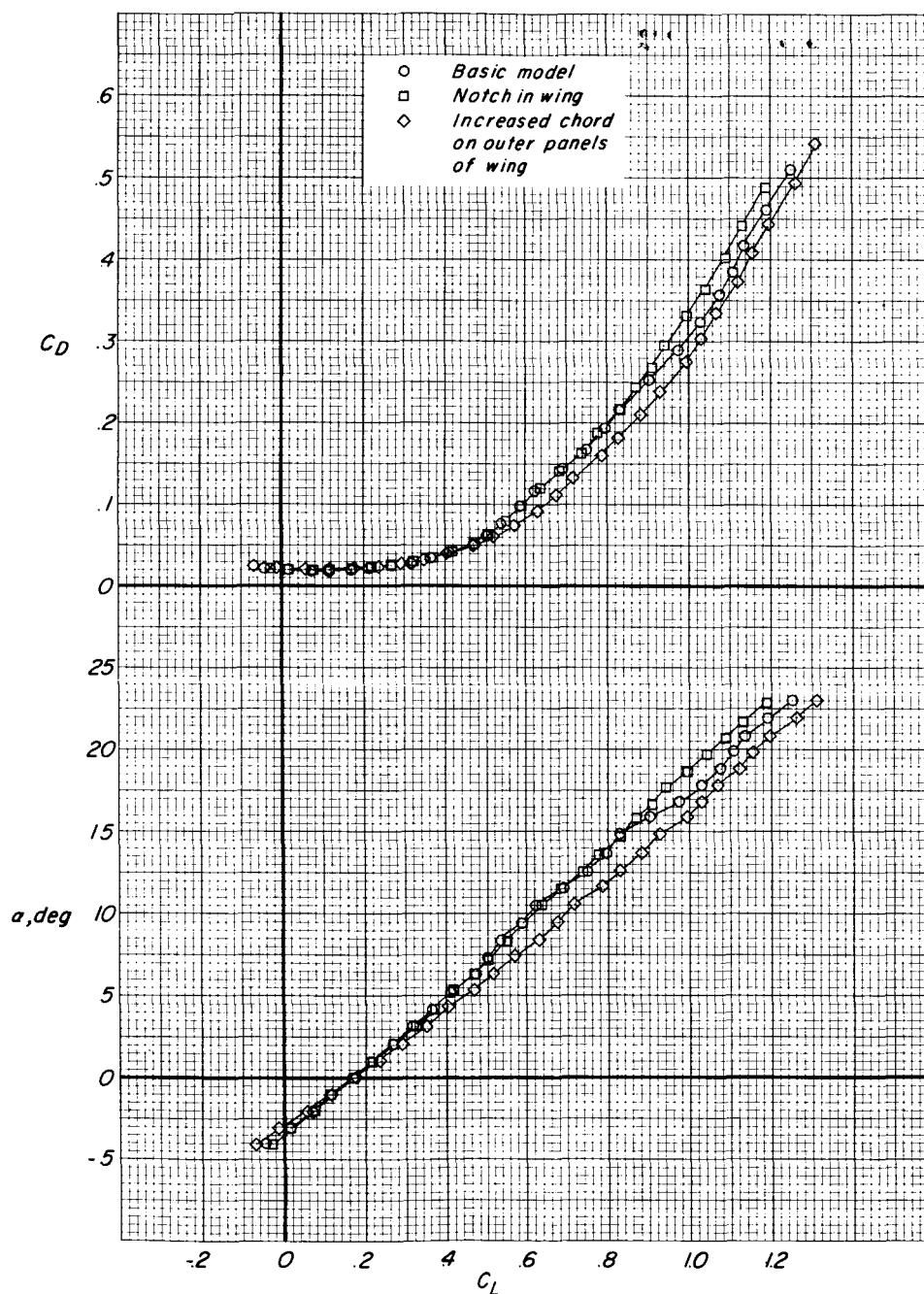


Figure 18.- Effect of a 1/4-inch-wide notch in the leading edge of the wing inner panels and effect of extending the chord of the outer panels forward 0.40c on the model with the wing swept back 25°. $i_t = 10^\circ$.

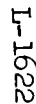


Figure 18.- Continued.

DECLASSIFIED

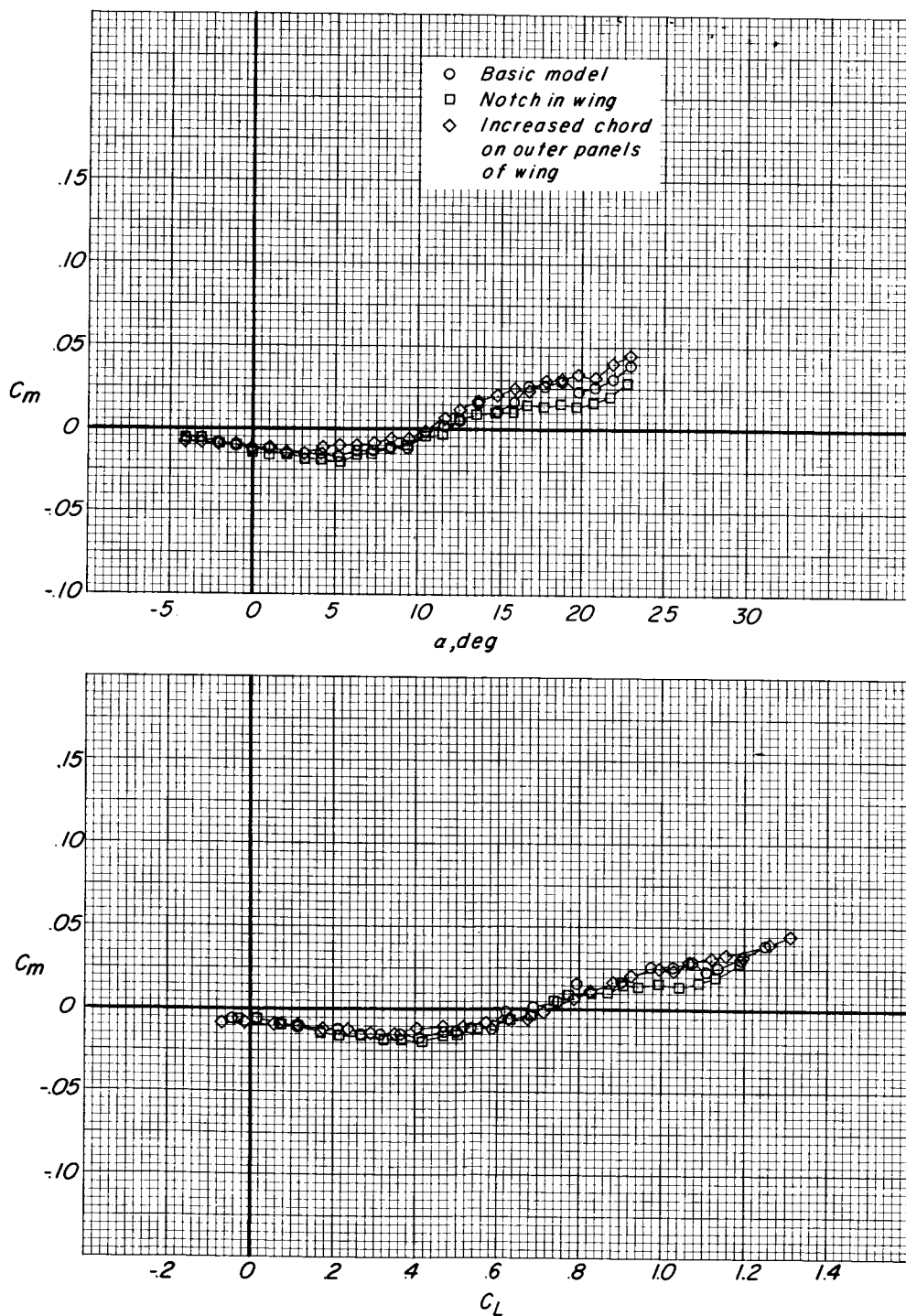
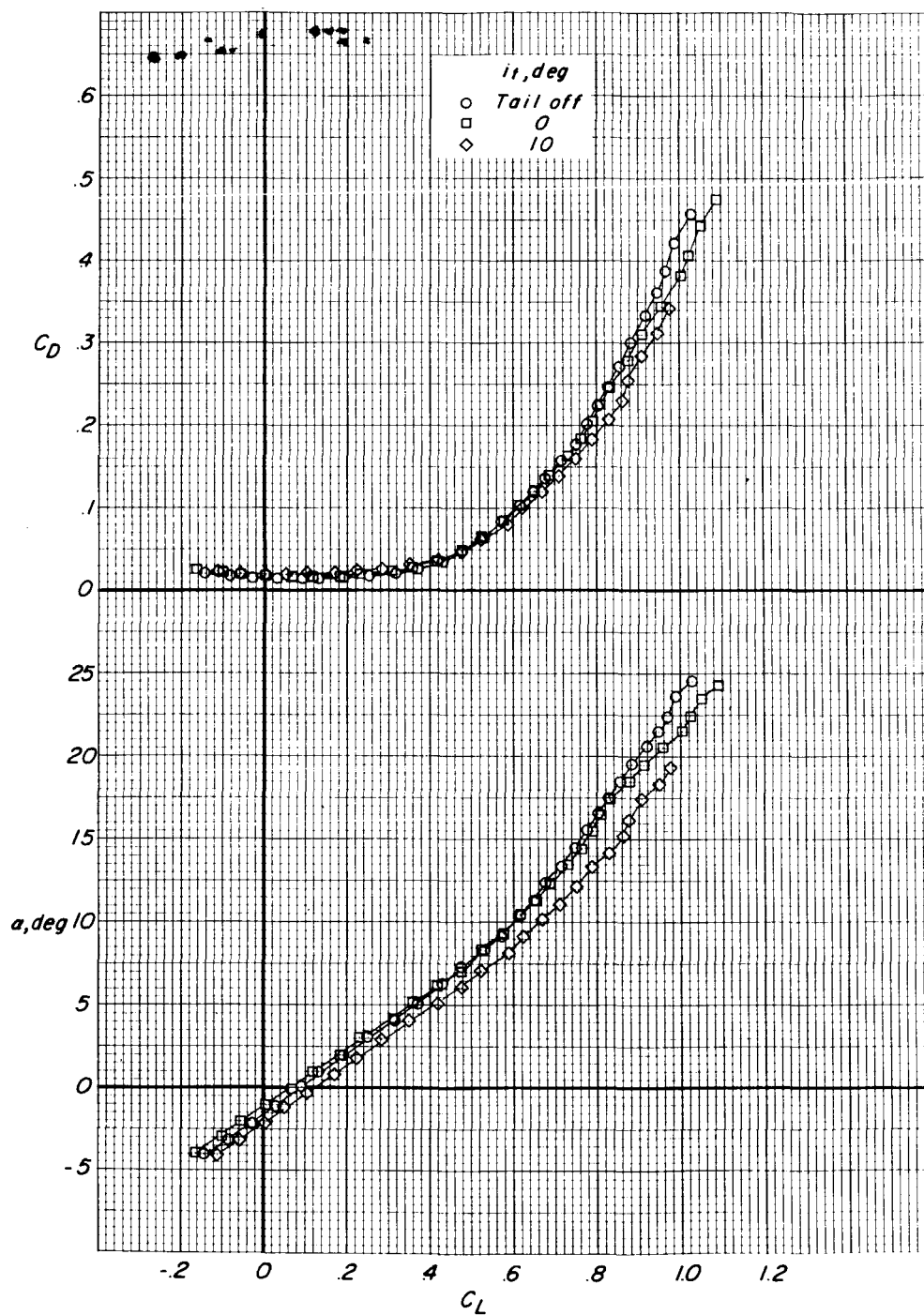


Figure 18.- Concluded.



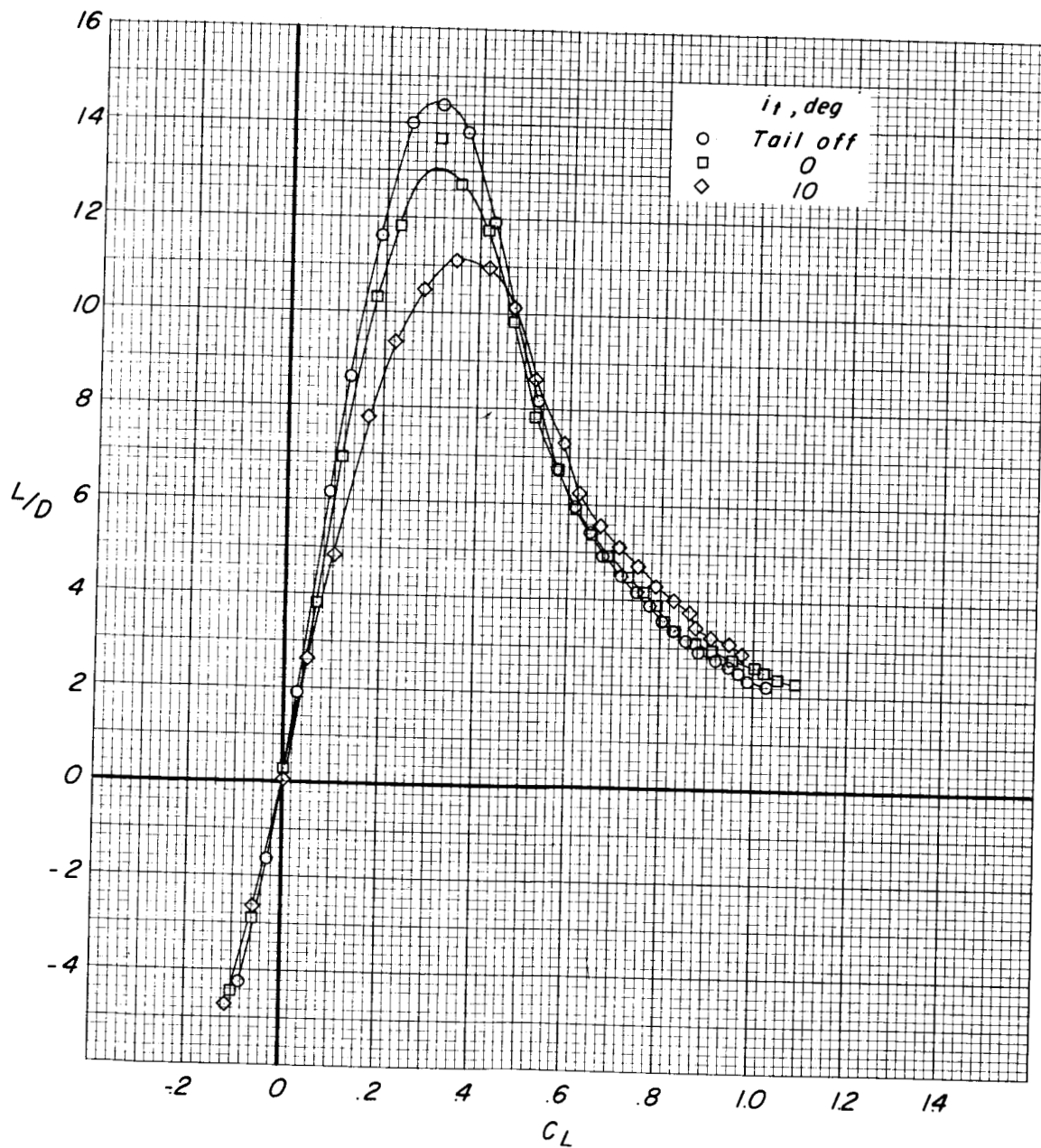


Figure 19.- Continued.



Figure 19.- Concluded.

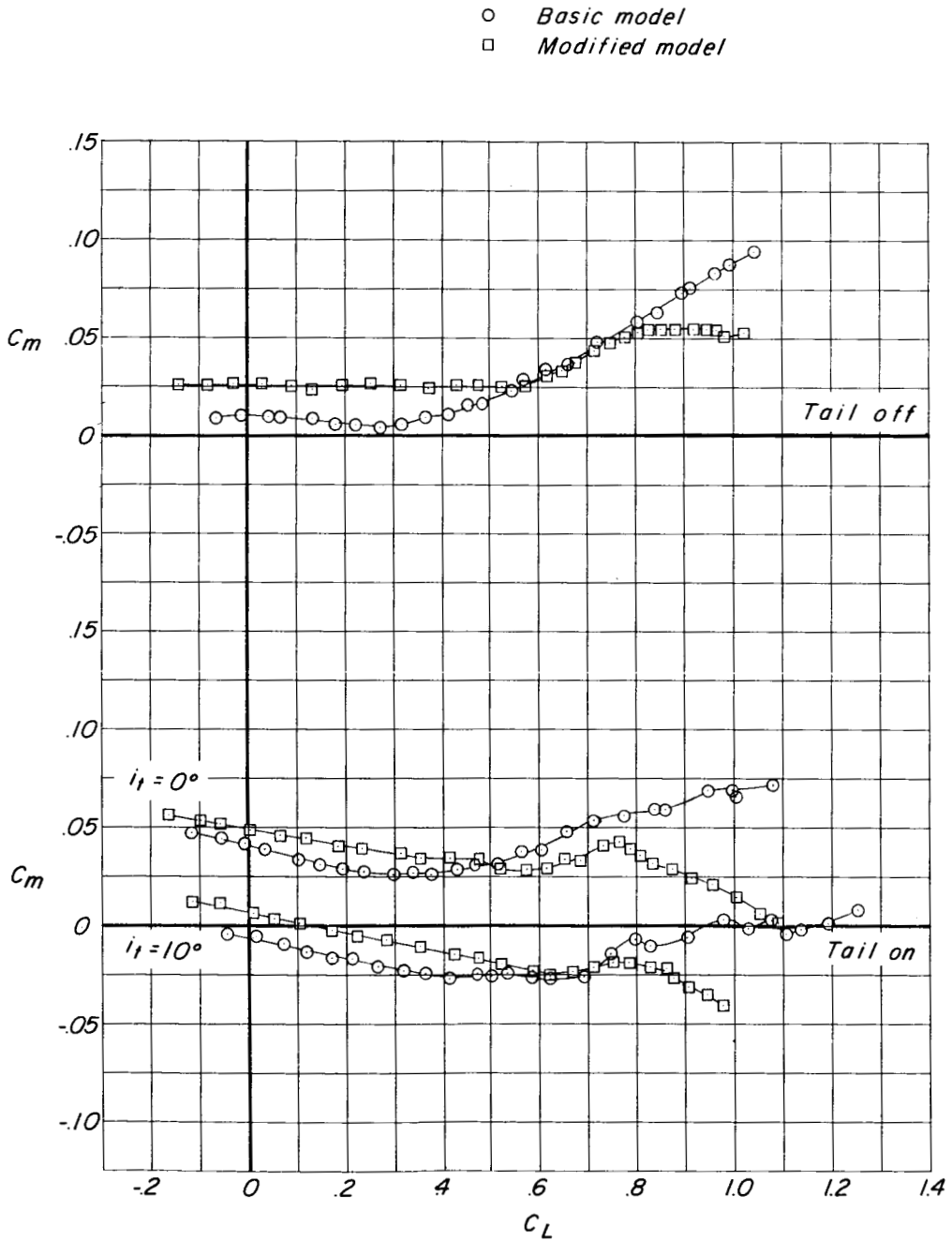


Figure 20.- Effect of elliptical planform wing leading edge on pitching moments of model with $\Lambda = 25^\circ$. Moment reference shifted to give approximately 5-percent static margin at low lift coefficients with the tail on.

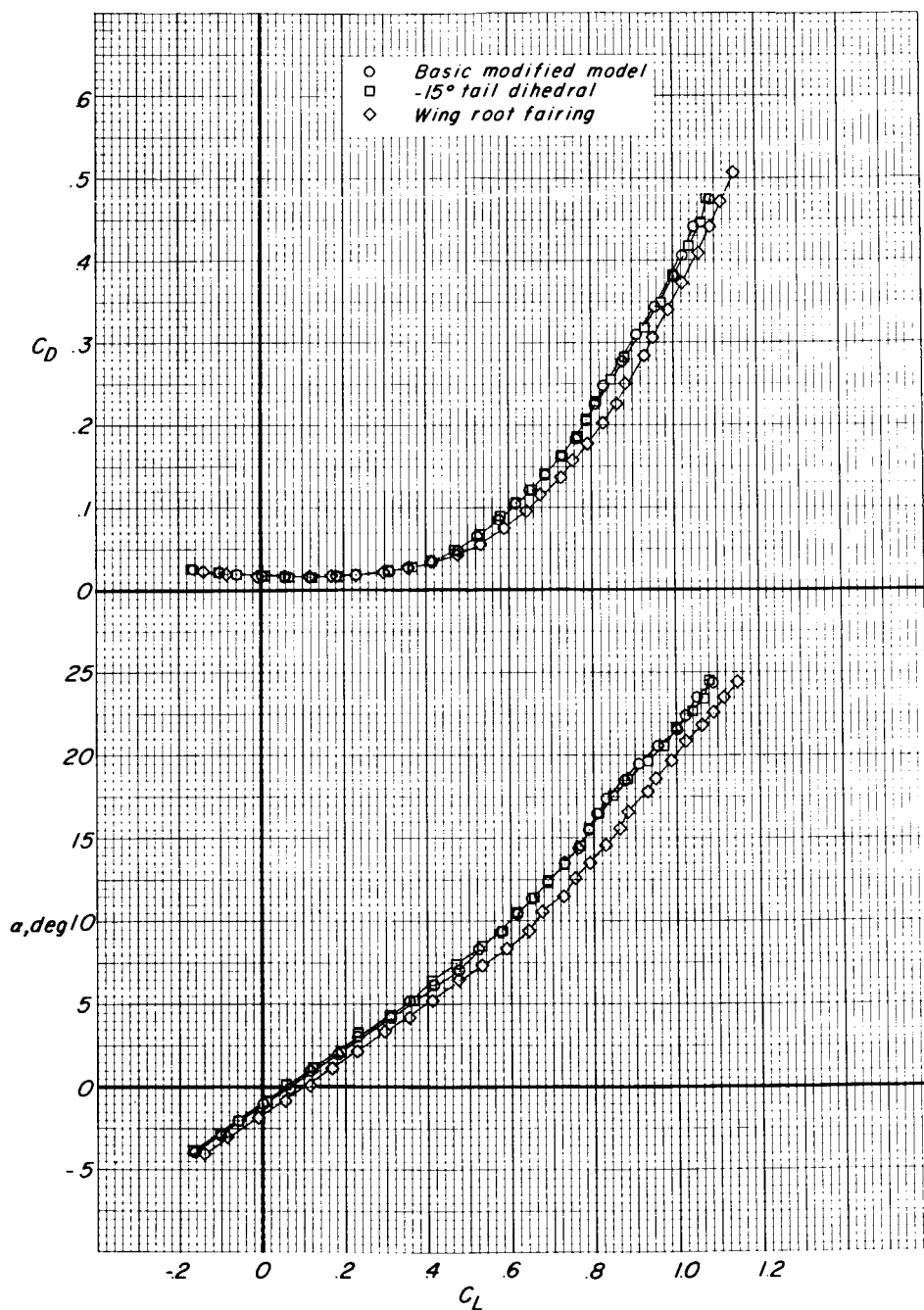


Figure 21.- Effect of -15° dihedral of the horizontal tail and effect of a leading-edge fillet at the wing root on the modified model having an elliptical planform leading edge and 25° sweepback of the outer wing panel. $i_t = 0^\circ$.

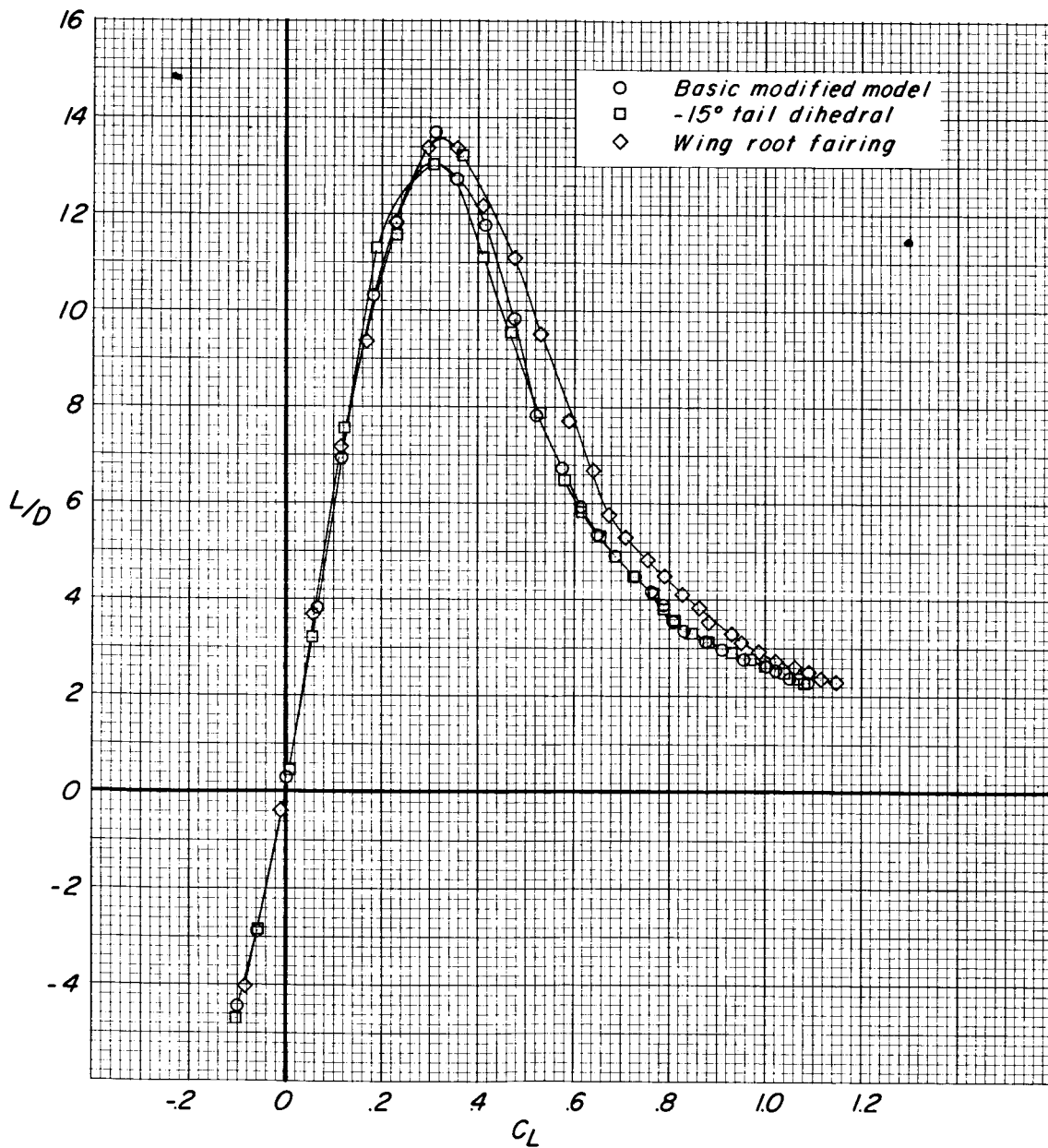


Figure 21.- Continued.

03 1039

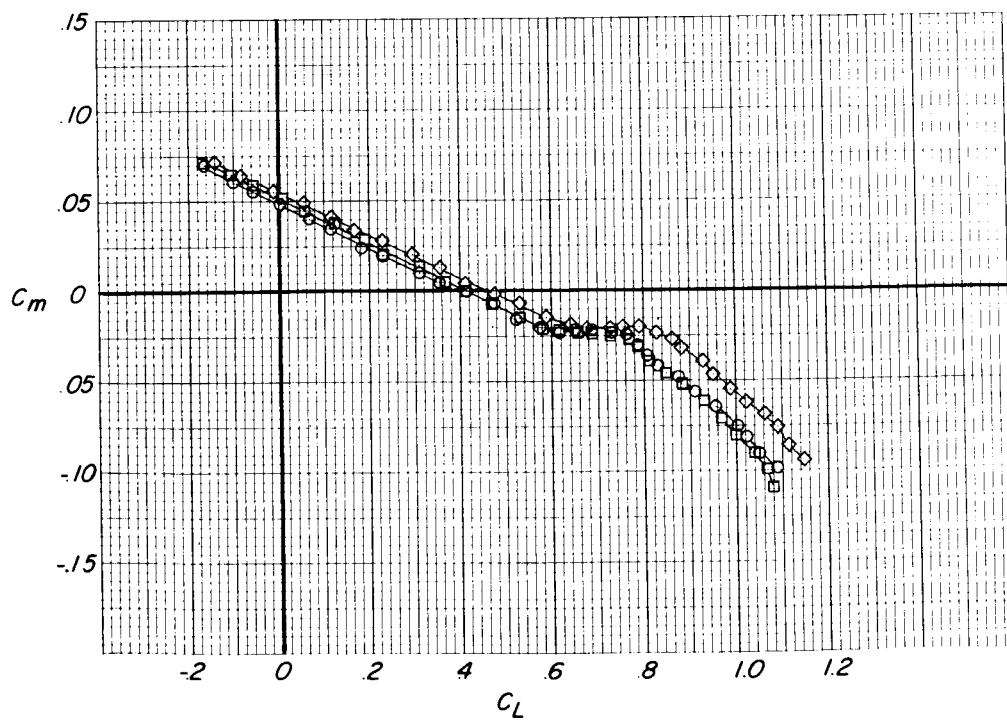
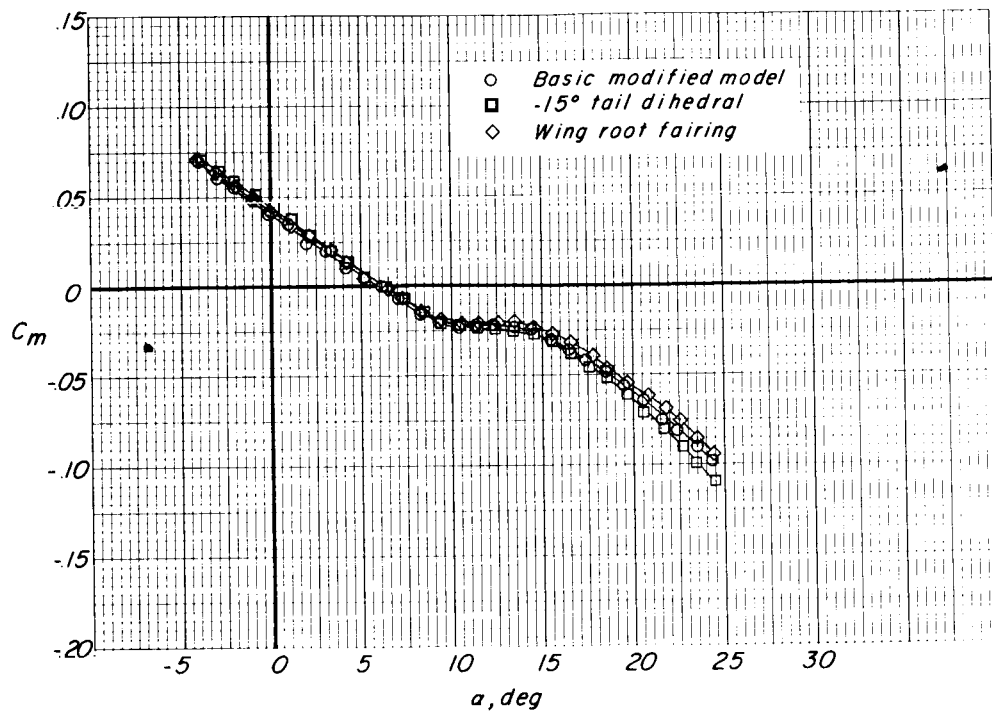


Figure 21.- Concluded.

AL

"The aeronautical and space activities of the United States shall be conducted so as to contribute . . . to the expansion of human knowledge of phenomena in the atmosphere and space. The Administration shall provide for the widest practicable and appropriate dissemination of information concerning its activities and the results thereof."

—NATIONAL AERONAUTICS AND SPACE ACT OF 1958

NASA SCIENTIFIC AND TECHNICAL PUBLICATIONS

TECHNICAL REPORTS: Scientific and technical information considered important, complete, and a lasting contribution to existing knowledge.

TECHNICAL NOTES: Information less broad in scope but nevertheless of importance as a contribution to existing knowledge.

TECHNICAL MEMORANDUMS: Information receiving limited distribution because of preliminary data, security classification, or other reasons.

CONTRACTOR REPORTS: Scientific and technical information generated under a NASA contract or grant and considered an important contribution to existing knowledge.

TECHNICAL TRANSLATIONS: Information published in a foreign language considered to merit NASA distribution in English.

SPECIAL PUBLICATIONS: Information derived from or of value to NASA activities. Publications include conference proceedings, monographs, data compilations, handbooks, sourcebooks, and special bibliographies.

TECHNOLOGY UTILIZATION PUBLICATIONS: Information on technology used by NASA that may be of particular interest in commercial and other non-aerospace applications. Publications include Tech Briefs, Technology Utilization Reports and Notes, and Technology Surveys.

Details on the availability of these publications may be obtained from:

SCIENTIFIC AND TECHNICAL INFORMATION DIVISION
NATIONAL AERONAUTICS AND SPACE ADMINISTRATION

Washington, D.C. 20546